Hierarchical differences in the encoding of sound and choice in the subcortical auditory system

Chase A. Mackey[1,2], Margit Dylla[2], Peter Bohlen[2], Jason Grigsby[2], Andrew Hrnicek[3], Jackson Mayfield[2] and Ramnarayan Ramachandran[2]
[1]Neuroscience Graduate Program, Vanderbilt University, Nashville, TN 37240
[2]Department of Hearing and Speech Sciences,
Vanderbilt University Medical Center, Nashville, TN 37212
[3]Department of Neurobiology and Anatomy, Wake Forest University Health Sciences,
Winston-Salem, NC 27101

Running title: Subcortical neural correlates of tone detection

Conflict of Interest Statement: The authors declare no conflict of interest

Author Contributions: RR designed the experiments. MD and PB collected data. MD, PB, JG, AH, CAM and JM analyzed the data under RR's supervision and guidance. RR and CAM wrote and edited the document, the other authors read and edited the document.

Data availability: Data and code are available upon request. Code is available at https://github.com/seemackey/master

Acknowledgements: This research was funded by a grant from the National Institutes of Health, RO1 DC 11092. CAM was supported by the Ruth Kirchstein F31 fellowship from NIDCD (F31 DC019823-02). The authors would like to thank Ms. Mary Feurtado and Dr. William Vaughan for help during surgery, Bruce and Roger Williams for hardware, Drs. Emilio Salinas, Jeff Schall, Richard Heitz, and Mark Wallace for helpful comments on an earlier version of the manuscript, Dr. Steve Lisberger and Mr. Scott Ruffner for the use of the FigureComposer software, and Ms. Laura Trice, and Drs. Troy Hackett and Jon Kaas for help with histology.

Contact Information:
Ramnarayan Ramachandran, Ph.D.
Department of Hearing and Speech Sciences
Vanderbilt University Medical Center
111 21st Ave S, WH 065
Nashville, TN 37212
(615) 322-4991 (phone)
(615) 343-0884 (FAX)
ramnarayan.ramachandran@vumc.org

Abstract (196 words)

Detection of sounds is a fundamental function of the auditory system. While studies of auditory cortex have gained substantial insight into detection performance using behaving animals, previous subcortical studies have mostly taken place under anesthesia, in passively listening animals, or have not measured performance at threshold. These limitations preclude direct comparisons between neuronal responses and behavior. To address this, we simultaneously measured auditory detection performance and single-unit activity in the inferior colliculus (IC) and cochlear nucleus (CN) in macaques. The spontaneous activity and response variability of CN neurons were higher than those observed for IC neurons. Signal detection theoretic methods revealed that the magnitude of responses of IC neurons provided more reliable estimates of psychometric threshold and slope compared to the responses of single CN neurons. However, pooling small populations of CN neurons provided reliable estimates of psychometric threshold and slope, suggesting sufficient information in CN population activity. Trial-by-trial correlations between spike count and behavioral response emerged 50-75 ms after sound onset for most IC neurons, but for few neurons in the CN. These results highlight hierarchical differences between neurometric-psychometric correlations in CN and IC, and have important implications for how subcortical information could be decoded.

New & Noteworthy

The cerebral cortex is widely recognized to play a role in sensory processing and decision-making. Accounts of the neural basis of auditory perception and its dysfunction are based on this idea. However, significantly less attention has been paid to midbrain and brainstem structures in this regard. Here we find that subcortical auditory neurons represent stimulus information sufficient for detection, and predict behavioral choice on a trial-by-trial basis.

Introduction:

A fundamental question in sensory neuroscience is how psychophysical capabilities of organisms are related to neuronal responses. Early studies characterized this relationship by comparing psychophysical and neuronal measures made at different times (e.g., Barlow et al. 1971; Tolhurst et al. 1983). Studies of the auditory system took this approach, characterizing neuronal responses to a variety of stimuli (Kiang et al. 1965; Goldberg and Brown 1969; Young and Sachs 1979), leading to models of auditory nerve fiber (ANF) response pooling to account for behaviors such as detection (e.g., Siebert 1965; Young and Barta 1985). However, subsequent neurometric analysis, which provides a more direct comparison between neuronal response and behavioral accuracy, demonstrated that thresholds of individual ANFs are much higher than behavioral thresholds (Delgutte 1995), motivating studies of signal detection in the central nervous system. Two candidate structures, the cochlear nuclei (CN) and inferior colliculi (IC), are near-obligate synapses where parallel neural pathways converge (see Oliver and Huerta 1992, Cant 1992, Moore et al. (2010), and Schreiner and Winer (2005) for reviews). Some studies of the IC have identified potential neural codes for detection (e.g., Wang et al. 2021), but these methods (when neural and behavioral measures are collected separately) preclude direct neuronal-behavioral comparison (Parker and Newsome 1998). Almost all previous CN and IC studies exhibit similar limitations, or have not measured performance near threshold (e.g., Ramachandran et al. 1999; Rhode et al. 2010; Ryan et al. 1984; Shaheen et al. 2021; Wang et al; 2021), leaving open fundamental questions about the role of subcortical structures in detection performance.

In contrast, many studies measuring performance at threshold in behaving animals have gained substantial insight into the neural basis of perception (e.g., Britten et al. 1992, 1996; Hernandez et al. 2000; Romo et al. 2002; Purushothaman and Bradley 2005; Nienborg and

50 Cumming 2009; Vazquez et al. 2012). These studies gained insight into two key aspects of
51 responses of sensory neurons: potential neural codes used for task performance, and choice-
52 related activity. Similar studies have been conducted in the auditory system, almost exclusively
53 in cortex, reporting potential neural codes, and correlates of behavioral choice (Christison-Lagay
54 et al. 2017; Francis et al. 2018; Lemus et al. 2009a,b; Niwa et al. 2012a,b), but it is unclear to
55 what degree this information is inherited from subcortical structures due to methodological
56 differences between cortical and subcortical studies. Similar subcortical studies have used a
57 classical conditioning paradigm (Kettner and Thompson 1980, 1985), which involves different
58 circuitry, and provides lower measures of accuracy than operant conditioning tasks (Behrens et
59 al. 2016), or have only measured responses in the CN (Lonsbury-Martin et al. 1987). Thus, it is
60 unclear whether CN and IC represent information sufficient for detection performance, choice-
61 related activity, and if they exhibit hierarchical differences in the encoding of these two
62 variables. This study capitalized on this opportunity by measuring single unit responses in the
63 CN and IC of rhesus macaques performing a reaction time sound detection task at threshold, with
64 the hypothesis that the encoding of sound and choice would improve hierarchically from CN to
65 IC. The findings reveal a hierarchy of sensory and choice-related information in the subcortical
66 auditory system.

67 **Methods:**

68 Experiments were conducted on four male rhesus monkeys (*Macaca mulatta*) that were
69 five (monkeys C, D) and eight (monkeys A, B) years of age at the start of these experiments and
70 were prepared for chronic experiments using standard techniques. All procedures were approved
71 by the Institutional Animal Care and Use Committees at Wake Forest University and Vanderbilt

72 University, and were in strict compliance with the guidelines for animal research established by
73 the National Institutes of Health.

74 Three surgical procedures were performed to prepare monkeys for this study. A head
75 holder was implanted in the first surgical procedure, and in the next two, craniotomies were
76 performed to access the CN and the IC, and recording chambers were implanted. All surgical
77 procedures were performed using sterile procedure and isoflurane anesthesia. During the first
78 surgical procedure, a head holder (Crist Instruments, Hagerstown, MD) was secured to the skull
79 using bone cement (Zimmer Inc., Warsaw, IN) and 8 mm long stainless steel screws (Synthes
80 Vet, West Chester, PA). The behavioral training on the detection task began after this surgery
81 (see below for details of the task). The other two surgeries implanted recording chambers (Crist
82 Instruments, Hagerstown, MD) on the skull around craniotomies at stereotaxically guided
83 locations. The recording chambers were angled to fit on the skull – the midbrain chamber was
84 tilted lateral 20˚, and the brainstem chamber was angled posterior 26˚ (similar to the approach for
85 the cerebellar flocculus, after Lisberger et al. 1994). The chambers were chosen with bases that
86 fit the cranial curvature, and secured to the skull using bone cement and screws. Pre- and
87 postsurgical analgesics, and, if necessary, antibiotics, were administered, and the monkey was
88 monitored carefully under veterinary supervision until complete recovery had occurred.

89 All experiments were conducted in double walled sound booths (IAC 1200, Industrial
90 Acoustics Corp., NY, and ER-247, Acoustic Systems, model ER 247) that measured 1.8m x
91 1.8m x 2m. During experiments, monkeys were seated in an acrylic primate chair custom
92 designed for their comfort and with no obstruction to sounds on either side of the head (Audio
93 chair, Crist Instrument Co., Hagerstown, MD). The monkeys' heads were positioned 90.1cm in
94 front of speakers placed level with the ears. The speakers (SA1 speaker, Madisound, WI, and

Rhyme Acoustics) could deliver frequencies between 50 Hz and 40 kHz, and were driven by linear amplifiers (SLA2, Applied Research Technologies, Rochester, NY) such that the sound level varied less than ±3 dB over the entire frequency range. All calibrations were performed with a 1/4" probe microphone (PS9200, ACO pacific, Belmont, CA) placed at the location of one of the ears of the head-fixed monkey.

Behavioral task:

Stimulus delivery, data acquisition, and reward delivery were controlled by a computer running OpenEx software (System 3, TDT Inc., Alachua, FL). The behavioral task and stimulus delivery mechanisms have been described in detail elsewhere (Dylla et al. 2013; Bohlen et al. 2014). Briefly, the monkeys were trained to detect 200 ms tone bursts with 10 ms rise and fall times. All training involved positive reinforcement. Monkeys initiated trials by pressing down on a lever (Model 829 Single Axis Hall Effect Joystick, P3America, San Diego, CA). When tones were presented after a variable hold time (600 – 1400 ms), monkeys were required to release the lever within a response window, usually extending up to 600 ms after the offset of the tone, for a fluid reward. The response window began with the onset of the stimulus; monkeys were free to respond even before stimulus offset. There were no penalties for not releasing the lever (miss), taken to indicate non-detection. On catch trials (~20% of the trials), monkeys were required to hold the lever pressed through the response duration, and were not rewarded for a correct reject response. Incorrect releases on catch trials (false alarms) were penalized with a timeout (6 – 10s) in which no tone was presented.

Signals were generated with a sampling rate of 97.6 kHz, and lever state was sampled at 24.4 kHz. Pure tones with sine onset phase, frequency f, and amplitude A were used as the signal to be detected. The value of A was varied such that the sound pressure level of each tone could

118 take values over a 90 dB range, going from -16 dB to 74 dB SPL in 3, 5 or 10 dB steps, and were
119 randomly interleaved. Each tone sound pressure level was repeated 15 to 30 times.
120 *Neuronal recording methods:*
121 A glass coated tungsten electrode (Alpha Omega Engineering, Alpharetta, GA; tip length
122 ~7-10 μm, diameter ~5 μm; Thomas Recording GmbH, tip impedance 3 – 4 MΩ) was placed in a
123 guide tube near the surface of the brain. The guide tube was advanced manually ~10 mm into the
124 brain; the electrode was advanced further into the brain by means of a remotely controlled
125 hydraulic micromanipulator (MO-97, Narishige Inc., Hampstead, NY). The electrode traveled
126 through the cortex to reach the IC, and through the cortex and cerebellum to reach the CN.
127 As the electrode was driven into the brain, bursts of noise were used as probe stimuli to
128 assess proximity to auditory structures. Proximity to CN or IC was indicated by changes in
129 background responses to the noise bursts. The IC was identified as the auditory structure
130 posterior to the superior colliculus (identified by superficial visual drive, deep layer eye
131 movement sensitivity, and response to visual and auditory stimuli) and anterior to the cerebellum
132 (identified by simple and complex spikes). Further criteria to identify IC (after Nelson et al.
133 2009) included: (i) short latencies (≤ 20 ms); (ii) reliable, non-habituating responses; and (iii)
134 identification of presence in tonotopic gradient (e.g. Merzenich and Reid 1974). The CN was
135 identified as the region of auditory responses medial to the flocculus (identified by simple and
136 complex spikes, and eye movement sensitivity to ipsiversive and downward eye movements
137 observed over the video monitor).
138 Once the electrode moved into the CN or IC, single units were isolated using tones (CN:
139 Spirou and Young 1991; Nelken and Young 1994; IC: Ramachandran et al. 1999; Davis 2002).
140 The electrode was advanced through the CN or IC until the signal from the electrode was

predominantly from one unit. Single units were verified based on visual inspection and the criterion that >99% of interspike intervals were at least 720 μs (after Nelson et al. 2009).

Once a single unit was isolated, its characteristic frequency (CF: the frequency with the lowest threshold) was manually estimated and used to derive the frequency tuning of the unit via a frequency response map (FRM). A FRM was obtained by measuring the responses of the unit to tones as a function of frequency and sound pressure level. Frequency was varied over a 2 or 4 octave range around the estimated CF in 100 logarithmically spaced steps and at multiple sound levels, starting near CF threshold values, and proceeding in 10 or 20 dB steps, similar to Rocchi and Ramachandran (2020). The FRM was used to estimate the CF of the unit online, which was then used as the frequency at which the monkey performed the detection task. FRMs were also used to classify the response type of the CN or IC units (CN: Evans and Nelson 1973; IC: Ramachandran et al. 1999). Sound pressure levels used for the FRMs ranged from 10 - 15 dB below estimated threshold to as high as 74 dB SPL. The raw waveform of the electrode signal and the waveforms of spikes that exceeded a threshold were sampled at 24.4 kHz and stored for offline analysis.

Behavioral Data Analysis:

Behavioral analyses were based on signal detection theoretic methods (Green and Swets 1966; Macmillan and Creelman 2005), implemented using MATLAB (MATLAB, RRID:nlx_153890; Mathworks, Natick, MA), and have been described previously (Dylla et al. 2013; Bohlen et al. 2014). Briefly, the false alarm rate (F) and the hit rate (H) for each tone level were calculated based on the number of trials at that sound level with lever releases within the response window and the total number of trials at that sound level. The behavioral accuracy was determined by:

$$p(c) = z^{-1}\left(\frac{(z(H) - z(F))}{2}\right),$$

where the *z(H)* and *z(F)* represent hit rate and false alarm rate in units of standard deviation of a standard normal distribution (*z*-score, norminv in MATLAB). The inverse function (z^{-1}) then converts a unique number of standard deviations of a standard normal distribution into a probability correct, a measure of behavioral accuracy (*p(c)*, normcdf in MATLAB). The *p(c)* was calculated for each tone level to create a psychometric function. Since the monkeys' false alarm rates influenced both the maximum performance and the estimate of chance performance at sound levels below threshold, psychometric functions did not always saturate at 0.5 and 1. To account for that, a Weibull cumulative distribution function (cdf) was fit to the psychometric function:

$$p(c)_{fit} = c - d * e^{-\left(\frac{level}{a}\right)^{b}} \text{ for level } \geq 0,$$

after the methods of Britten et al. (1992) and Palmer et al. (2007), where *level* represents the tone sound pressure level in dB SPL, *a* and *b* represent the threshold and slope parameters, *c* and *d* represent the ceiling and floor saturation rates that could differ from 1 and 0.5, respectively, and *e* is the base of natural logarithms (*e*=2.71828). To account for the sound pressure levels below 0 dB SPL, the data were translated upward by the lowest sound pressure level used, fit with the Weibull cdf, and then the thresholds were translated back to the original sound pressure levels. Threshold was calculated from the fit as that tone level that evoked p(c) = 0.76, and was close to the value of *a*. In all cases, reaction time (RT) was also computed, based on the time of the lever release. RT was computed as follows:

Reaction time = time of lever release - time of tone onset

Neurophysiological Data Analysis:

186 Offline, the neurophysiological data were spike sorted using a Bayesian spike-sorting
187 algorithm (OpenSorter, TDT, Alachua, FL), which were then used for all further analyses. The
188 spike-sorter identified spikes based on a manually set threshold, and then clustered the voltage
189 waveforms exceeding the threshold based on Bayesian classification schemes. The validity of the
190 clustering was further checked based on spike shape and distribution of interspike intervals.
191 Spikes occurring across the entire 200 ms tone duration in the FRMs were used to classify units
192 into response types (IC: Ramachandran et al. 1999; CN: Evans and Nelson 1973), and to
193 calculate the CF. The calculated CF values matched the online CF estimates to within a sixteenth
194 of an octave more than 98% of the time and did not represent a source of error.
195 Initial analyses determined the magnitude of the response evoked by each stimulus. For
196 each trial, the response was computed by cumulating the number of spikes evoked by the tone.
197 Thus, a distribution of responses was created for each tone level, including the no tone condition
198 on catch trials. These distributions were used to determine the behavioral accuracy predicted by
199 the ideal observer based on neuronal responses using traditional Receiver Operating
200 Characteristic (ROC) analyses (after Barlow et al. 1971; Tolhurst et al. 1983; Britten et al. 1992;
201 Palmer et al. 2007). Briefly, the distribution of the responses on catch trials were compared to the
202 distributions of responses on signal trials to determine the probability of an ideal observer
203 determining that the responses under the two conditions were different. Such neurometric
204 probabilities were computed at each sound pressure level to generate a neurometric function
205 (after Britten et al. 1992; Palmer et al. 2007). The neurometric functions were fit with Weibull
206 cdf using the equation described above, and neurometric thresholds and slopes were derived
207 from the parameters of the Weibull cdf.

The spiking response on each trial was regressed against the RT on that trial to determine the correlation between response magnitude and RT. Since response latencies can also be a contributor to RT, response latencies were calculated on a trial-by-trial basis using the method described by Rowland et al. (2007). Briefly, spike counts were cumulated from the beginning of the trial, and inflections in the spike count were used to determine response latency and time of response offset on each trial. Both variables were regressed against RT to determine the correlation between a measure of response timing and RT.

The dependence of the neuronal responses to behavioral choice was determined using the choice probability metric (Britten et al. 1996; Cook and Maunsell 2002), and was labeled the detect probability (DP), similar to Cook and Maunsell (2002). When three or more correct and incorrect responses were present, the responses on correct and incorrect trials at the same sound pressure level were compared using ROC analysis. The DP measure calculated the probability with which an ideal observer could predict detection accuracy at that tone sound pressure level based on the trial-by-trial response fluctuations. A DP of 0.5 indicates that the neuronal responses on correct and incorrect trials were not significantly different to an ideal observer, DP > 0.5 indicates that responses were usually larger on correct trials relative to incorrect trials, and DP < 0.5 suggests that responses on incorrect trials were larger than responses on correct trials. Kang and Maunsell (2012) identified potential confounds in calculation of DP (e.g. sample size asymmetry between correct and incorrect responses). Mirroring the methods they described, we sampled neuronal responses 1,000 times with replacement to determine the DP and its significance by permutation test (1,000 repetitions).

When three or more correct and incorrect responses were available at more than one sound pressure level (i.e., the dynamic range was captured by more than one sound pressure

231 level), a grand DP was computed by across all the levels after z-scoring. We also verified that
232 where only analysis of responses at one sound pressure level was possible, the z-scores and
233 response magnitude based ROC analyses were not different from each other.

234 *Pooling analysis*

235 A pooling model was created to assess the effect of converging CN responses on
236 neurometric performance, to formalize assumptions about how inputs to the IC could lead to
237 responses observed in the IC. The inputs to the model were responses of actual CN neurons
238 recorded. Because the population of units had CF that varied over the audiometric range, unit
239 responses as a function of sound level were normalized such that neurometric threshold reflected
240 the difference between the original neurometric threshold and psychometric threshold. The
241 number of inputs to the model was varied to test the effect of pool size, and determine the pool
242 size that was sufficient to match psychometric performance. The inputs to the model were
243 sampled 1000 times with replacement, and summed, (similar to Britten et al. 1992). The summed
244 responses were subject to ROC analysis described above, to attain neurometric accuracy of the
245 population.

246 *Statistical analysis of similarity between neurometric and psychometric parameters:*

247 Since a goal of this study was to determine neurometric-psychometric correspondences,
248 we used bootstrap methods. The distributions of neuronal and behavioral responses at each tone
249 level were resampled 1000 times to create 1000 distributions of neuronal and behavioral
250 responses at that tone level. This was repeated for each tone level. Thus, the behavioral and
251 neuronal responses as a function of tone level were resampled with replacement to create 1000
252 different response vs. level functions and hit rate vs. tone level functions. Signal detection
253 theoretic and ROC analyses were performed on each of the resampled hit rate vs. tone level

254 functions and response vs. level functions to derive one thousand neurometric and psychometric
255 functions. Each of the neurometric and psychometric functions was then fit with Weibull cdfs to
256 derive distributions of threshold and slope for psychometric and neurometric conditions. The
257 95% confidence limits of these distributions (confidence intervals, CI) were then calculated. The
258 CIs were compared across similar psychometric and neurometric parameters for overlap. These
259 distributions were then compared statistically to determine differences in psychometric and
260 neurometric parameter pairs at the 5% level using a Wilcoxon signed rank sum test.

261 *Histological analyses*

262 All four of the monkeys were euthanized, but we were unable to place markers (lesions or
263 tracer injections at physiologically characterized sites). The brains were extracted (fresh in the
264 case of monkey A and post fixed, and after transcardial perfusion with 4% paraformaldehyde
265 following euthanasia and exsanguination in other monkeys). The subcortical regions were
266 blocked caudal to the medial geniculate nucleus to include both the IC and CN. The brain blocks
267 were allowed to sink in a 30% solution of sucrose in phosphate buffer (pH 7.2 – 7.4) and cut into
268 50 µm sections. The sections were stained with cytochrome oxidase (CO, Millipore Inc.,
269 Billerica, MA) and then mounted on slides, or mounted on slides and stained with thionin
270 (Sigma, St. Louis, MO). The thionin stained sections were used to identify subdivisions of the
271 CN and the IC. Figure 1 shows sections through the IC and CN in monkeys A and B stained with
272 CO (an example from monkey D is shown in Rocchi and Ramachandran (2020)). Tracks were
273 found in both structures (ovals in Figure 1) and confirmed based on adjacent sections. Fewer
274 tracks were found in the CN than in the IC, but could be attributed to the 26˚ anterior-posterior
275 electrode angle being viewed through nearly coronal sections. Tracks were found throughout the
276 rostrocaudal extent of the IC and the CN, including tracks through the dorsal CN (DCN),

277 providing anatomical confirmation that the recordings in these macaques were indeed from the
278 IC and the CN. The tracks in the IC were found passing through the central nucleus, consistent
279 with the recording approach of looking for tuned auditory responses. Tracks were found to
280 extend throughout the dorsoventral extent of the central nucleus of the IC, indicating that the
281 electrodes traversed a majority of the representation of the frequency extent, consistent with the
282 range of unit CFs measured (see Figures 4A and 4B). Electrode tracks were also found
283 throughout the anterior-posterior extent of the CN, indicating evidence of sampling throughout
284 the frequency extent in the CN also (also see Figures 7A and 7B).

285 **Results:**

286 *Basic response properties*

287 The responses of 108 single units with complete psychometric and neurometric data were
288 studied in the IC of four monkeys (A, n=25; B, n=36; C, n=9; D, n=38). Responses were also
289 obtained from 92 single units with complete psychometric and neurometric functions and
290 sufficient number of trials in the CN in the same monkeys (A, n=29; B, n=44; C, n=1; D, n=18).
291 As observed in multiple species, the IC had a tonotopic region in which the CF of single units
292 increased progressively as the electrode traveled dorsolateral to ventromedial (Reviewed in
293 Oliver and Huerta (1992); Schreiner and Winer (2005); and Moore et al. (2010)); the CN had
294 multiple tonotopic fields. All the IC data presented in this report were obtained in the tonotopic
295 region of the IC, most likely the central nucleus of the IC; these were confirmed by the majority
296 of tracks traversing through the central nucleus of the IC (see Figure 1). The physiological
297 signatures (short latency auditory responses, the tonotopic gradient, and the FRM types) were
298 consistent with the recordings being from the central nucleus of the IC (ICC), and from all

299 divisions of the CN. The majority of the CN units were obtained in the anterior two-thirds of the
300 structure (putative ventral CN).

301 The CFs of the units used in this manuscript ranged between 200 Hz and 32 kHz for IC
302 units and between 300 Hz and 34 kHz for CN units; the sample of IC units in monkeys C and D
303 had predominantly low CFs because those monkeys were also used in studies of neuronal
304 encoding of vowels, which are lower frequency signals. IC units were classified, based on their
305 binaural diotic frequency response map (FRM) as IC type V (V-shaped excitatory FRM about
306 CF, n=68) or IC type I (V-shaped excitatory FRM about CF, with inhibition flanking excitation,
307 n=35) units (after Ramachandran et al. 1999). The responses of a small number of type O units
308 (n=5, after Ramachandran et al. 1999), whose responses to CF tones at high sound pressure
309 levels fell below spontaneous activity, were recorded, consistent with previous reports (Nelson et
310 al. 2009). CN units were classified into CN type I units (the Roman numeral 1, having V-shaped
311 excitatory FRMs with no inhibitiory responses, n=44), CN type III units (Roman numeral 3, V-
312 shaped excitatory FRM and flanking frequency regions of inhibition, n=37), CN type IV units
313 (Roman numeral 4, low sound level excitation at CF, and inhibitory responses at higher levels,
314 n=6), and CN type V units (Roman numeral 5, inhibition at all responsive frequencies and sound
315 levels, n=4) based on existing classification methods (e.g., Evans and Nelson 1973; Shofner and
316 Young 1985).

317 Figure 2 shows some exemplar waveforms and some basic response measures in the IC
318 and the CN. Figure 2A shows waveforms obtained during recordings of a single unit in the IC
319 and one during the recordings of a single unit in the CN. As expected for single units, the
320 amplitude was very stable over time for all units classified as single units. Figure 2B shows the
321 distribution of baseline/spontaneous activity (activity when sound stimuli were not presented) in

322 the IC and in the CN (filled and open bars respectively). The mean spike count over the 200 ms
323 stimulus duration on catch trials were calculated and scaled to provide the spontaneous firing
324 rates. There was not a significant difference in the spontaneous rates depending on unit type for
325 either the CN or the IC (Kruskal Wallis test, $p>0.05$), so the spontaneous rates were combined
326 across unit types. The spontaneous rates of CN and IC units took values over the similar ranges
327 (IC: 1.8 – 60.2 spikes/s; CN: 1.2 – 69.8 spikes/s), but their distributions were very different.
328 Spontaneous rates of IC units tended to be lower (mean = 18.6 spikes/s, median =13.65 spikes/s).
329 CN unit spontaneous rates tended to be higher, with a mean of 30.3 spikes/s, and a median of 30
330 spikes/s. The ranges of spontaneous firing rates of CN and IC units were consistent with the
331 published values or the ranges in unanesthetized animals (e.g., IC: Ramachandran et al. 1999;
332 CN: Evans and Nelson 1973). The spontaneous activity in the CN and IC were significantly
333 different from each other (Wilcoxon ranksum test, $Z=5.53$, $p=1.8\text{x}10^{-8}$).
334 The variability of neuronal responses is a crucial determinant of stimulus encoding.
335 Figures 2C and D show the relationship between the standard deviation (SD) of the firing rate
336 and the mean firing rate in response to the tones at CF for CN and IC units, respectively. Both
337 figures show that variability of the firing rate was related to the mean, consistent with findings in
338 the auditory system (e.g., May and Huang 1997; Reiss et al. 2011). For both CN and IC, the
339 relationship between mean and standard deviation was best fit with a power law function (grey
340 and black curves in Figures 2B and C respectively). However, there are differences between the
341 CN and IC. The maximum mean response of IC units (maximum = 260 spikes/s) was lower than
342 that of CN units (maximum = 314 spikes/s). More noteworthy was that the standard deviation (or
343 variability) of IC firing rates was lower than that of CN firing rates. Thus, CN units had higher
344 baseline activity, and higher variability in their activity than IC units. Thus, exceeding the

345 baseline based on statistical criterion would take larger changes in the mean firing rates of CN
346 units as compared to IC units, suggesting that neurometric thresholds of CN units would be
347 higher than that of IC units.

348 *Responses in the inferior colliculus (IC)*

349 Behavioral thresholds to tones were obtained from all four monkeys prior to
350 neurophysiological measurements. The audiometric thresholds of the monkeys have been
351 published in earlier papers (Dylla et al. 2013; Bohlen et al. 2014) and were not different from the
352 published audiometric functions from other labs (e.g., Stebbins et al. 1966; Pfings et al. 1975).
353 The psychometric thresholds during physiological recordings did not differ from the baseline
354 psychometric thresholds obtained prior to chamber implantation and neurophsyiological
355 measurements (Dylla et al. 2013). The responses of IC type O units were excluded from analysis
356 relative to detection behavior due to their posited role in sound localization (Davis et al. 2003).

357 Figure 3 shows the responses of single units recorded in the IC of awake and behaving
358 monkeys to CF tones as a function of tone level, and the calculation of neurometric functions and
359 parameters. Figures 3A and B show spike count as a function of the CF tone sound pressure level
360 for an IC type V (CF=2.2 kHz) and IC type I unit (CF=25.6 kHz). The relationship between
361 spike count and tone level for these unit types could be monotonic or nonmonotonic, but never
362 fell below spontaneous rate (solid line, Figure 3A and B). The distribution of responses at each
363 tone level was compared with the responses on catch trials (colored and white bars, respectively,
364 Figures 3C and D). At low tone levels (e.g., -6 dB SPL), the units were unresponsive to the CF
365 tone, with responses during stimulus duration matching those on catch trials when no tone was
366 presented. At high tone levels (e.g., 54 dB SPL), the units' responses to the CF tone exceeded the
367 magnitude of the responses on catch trials. The increasing responsiveness to the tone created

368 separation between the catch trial and the signal response distributions (Figure 3C and D). A
369 receiver-operating characteristic (ROC) was created by systematically defining criteria over the
370 range of spontaneous and signal response distributions to create false alarm and hit rates. The
371 area under the ROC curve is an ideal observer's probability of being correct in a binary choice
372 task (tone present vs. not present), based on the neural firing rate during the tone ("neurometric",
373 open symbols, Figure 3E and F). These neurometric functions were fit with Weibull cdfs (dashed
374 curve, Figure 3E and F) as described in the Methods section. To directly compare these with
375 behavioral performance, simultaneously measured psychometric functions (filled circles) and
376 their Weibull cdf fit (solid curve) are also shown in the same panels. The sound pressure level
377 that evoked $p(c)_{fit} = 0.76$ was considered the threshold (solid and dashed vertical lines indicate
378 psychometric and neurometric thresholds respectively, Figures 3E and F).

379 The neurometric functions for the exemplars were remarkably similar to the
380 psychometric functions (IC type V: neurometric: a=20.77, b=3.32; psychometric: a=19.77,
381 b=3.28; IC type I: neurometric: a=24.6, b=4.45; psychometric: a=26.8, b=4.5). In both exemplar
382 cases, the neurometric and psychometric parameters (thresholds and slopes) were not
383 significantly different from each other, determined via Monte-Carlo methods (see Methods; IC
384 type V: threshold: p= 0.427; slope: p=0.226; IC type I: threshold: p= 0.513; slope: p= 0.39). The
385 similarity between the psychometric and neurometric parameters was a very common feature of
386 the data obtained in the IC.

387 Figure 4 plots thresholds against the characteristic frequency for all IC type V and I units
388 across all the monkeys. Figure 4A (left) plots the psychometric thresholds against the frequency
389 of the target tone (the CF of the unit being recorded). The different symbols show the data from
390 the different monkeys. The data shows that units with a large range of CFs were recorded in all

391 monkeys, that the behavioral thresholds showed a U-shaped contour that has been observed in
392 audiograms of macaques (e.g., Stebbins et al. 1966; Dylla et al. 2013). Figure 4A (right) shows
393 neurometric thresholds as a function of unit CF for monkeys A – D using symbols similar to the
394 behavioral panel. The neurometric thresholds also fell along a U-shaped contour similar to the
395 psychometric threshold, though IC neurometric thresholds took a larger range of values. To more
396 easily visualize differences in psychometric and neurometric thresholds, we plotted the
397 difference between psychometric and neurometric threshold for each unit against the unit CF
398 (Figure 4B). The large number of units with low CF (< 1 kHz) reflects data collected during a
399 study of the neuronal representation of vowels (low frequency sounds). The figure shows that the
400 observation of similarity of psychometric and neurometric thresholds were not restricted to a
401 single frequency range but were a general feature across CFs. Figure 4B also revealed that some
402 units had higher thresholds than behavior.

403 Figure 4C plots IC neurometric thresholds against simultaneously measured
404 psychometric thresholds. There were no significant differences in the relationship between
405 psychometric and neurometic thresholds as a function of unit type, so units of both major types
406 are shown together. Filled and unfilled circles indicate units whose neurometric thresholds were
407 and were not significantly different from the psychometric threshold (see Methods), respectively
408 (Figure 4C). The clustering of circles around the diagonal indicates that neurometric thresholds
409 for many IC neurons were around and not significantly different from psychometric thresholds.
410 There was a significant correlation between individual neurometric and psychometric thresholds
411 ($r=0.625$, $p<0.01$), strengthening the idea that the strong correlation is at the single unit level, not
412 just on the average. Such correlations could arise out of common factors. Psychometric
413 thresholds in primates vary with tone frequency (e.g., Green et al. 1966; Pfingst et al. 1975;

414 Dylla et al. 2013), as do neuronal thresholds in various auditory regions (e.g., IC: Ramachandran
415 et al. 1999). When multiple regression was used with CF as covariate, the partial correlation
416 between psychometric and neurometric threshold was much reduced and not significant
417 (r=0.155, *p*=0.119). The range of neurometric thresholds observed in Figure 4C is due to the
418 sample containing units with CFs that spanned nearly the entire audiometric range, and thus
419 showing a threshold ranging from ~-5 to 35 dB SPL. The histogram of threshold differences
420 shows a strong mode around 0, and ~75% of units (76/102) had threshold differences within ±10
421 dB (Figure 4C). The median was close to zero (0.5 dB): on the average, the psychometric and IC
422 neurometric thresholds were similar in value, and were not significantly different from each
423 other (Wilcoxon signed rank sum test, Z=0.89, *p*=0.374).

424 For IC unit responses to adequately represent behavioral performance, IC neurometric
425 functions need to account for both threshold and shape (slope) of the psychometric functions
426 (Parker and Newsome 1998). Since the slope parameter of a Weibull cdf depends on threshold,
427 the slope parameter *b* was not used; rather, the slope was measured as the linear slope of the
428 dynamic portion of the neurometric or psychometric function (10 – 90% of the range). Figure 4D
429 shows a comparison of the psychometric and neurometric function slopes. The data points are
430 scattered around the diagonal line of equal slopes, and with much more variability than that
431 observed for thresholds (compare Figures 4C and D). As with thresholds, the relationship
432 between psychometric and neurometric slopes was independent of CF and response type. As
433 with thresholds, resampling methods were used to compare individual psychometric and
434 neurometric thresholds, and units with significantly different slopes are shown with filled circles.
435 The psychometric and neurometric slopes were significantly correlated ($r = 0.497$, $p < 0.05$),

436 suggesting good match between the two slopes at the single unit level. The slope difference
437 histogram reflects the same trend by a broad distribution centered on 0 (median = -0.002/dB).
438 *Responses in the cochlear nucleus (CN)*
439 The strong match between the responses of IC units and behavioral responses could be
440 due to either: (i) behaviorally matched neuronal responses that input to the IC; or (ii) synthesis in
441 the IC, *de novo* or via cortical efferents. To separate the two possibilities, responses were
442 obtained in the CN during the same task. Since the responses were uniform across locations
443 within the CN, the data were combined across all CN recording locations. As in the case of the
444 IC, psychometric thresholds during neurophysiological experiments did not deviate significantly
445 from baseline psychometric thresholds at similar frequencies.
446 Figure 5 shows the responses of an exemplar CN type I unit (Figures 5A, C, E) and CN
447 type III unit (Figures 5B, D, F) and the ROC analysis in a manner similar to Figure 2. The
448 response magnitudes of CN were monotonic or weakly nonmontonic as a function of CF-tone
449 sound pressure level (Figures 5A and B). As with IC units, the distributions of CN responses on
450 signal and catch trials (Figures 5 C, D) were converted, using ROC analysis, into neurometric
451 functions (Figures 5 E and F). The neurometric functions (open circles) were fit with a Weibull
452 cdf (dashed curve), and are shown along with the simultaneously obtained psychometric function
453 (filled circles) and its Weibull cdf fit (solid curve). Threshold and slope parameters were
454 extracted for both data sets. In both examples, the psychometric and neurometric functions
455 appeared very different and the fit parameters were different (CN type I: neurometric: a=4.2,
456 b=3.43; psychometric: a=-2.7, b=4.94; CN type III: neurometric: a=25.1, b=6.17; psychometric:
457 a=17.7, b=4.8). The psychometric and neurometric thresholds for the exemplar CN units were
458 significantly different from each other as assessed by Monte-Carlo methods (see Methods; CN

459 type I: p= 0.0134; CN type III: p= 0.009). However, the psychometric slopes for the type I unit
460 were significantly different from (higher than) the neurometric slope (slope: p= 0.0099), the
461 psychometric and CN type III neurometric slopes were not significantly different (slope: p=
462 0.319).

463 Figure 6 shows a comparison of psychometric and neurometric parameters while
464 recordings were made in the CN using a format similar to Figure 4. Figure 6A (left) shows
465 behavioral thresholds during recordings in the CN. The threshold trends were similar to those in
466 Figure 4, and are in general, similar to macaque audiograms (e.g., Stebbins et al. 1966; Pfingst et
467 al. 1978; Dylla et al. 2013). Figure 6A (right) shows CN neurometric thresholds as a function of
468 CF. Thresholds did not vary with the identity of the monkey, and can be seen by comparing the
469 relative locations of the different symbols. In contrast to the IC data in Figure 4A(right), the CN
470 neurometric thresholds were biased to higher tone levels (Figure 6A, right). The differences
471 between psychometric and neurometric threshold were plotted against the unit CF for easy
472 visualization (Figure 6B, same format as Figure 4B). Threshold differences between
473 psychometric and neurometric functions in the CN and IC were significantly different (Wilcoxon
474 ranksum test, Z=8.831, p<0.00001). The difference between psychometric and neurometric
475 thresholds for CN units (circles) were not related to the CF of the unit, and across the entire
476 range of frequencies sampled, units in the CN had neurometric thresholds that were higher than
477 psychometric threshold (Figure 6B). Note that the psychometric-neurometric threshold
478 differences for the majority of CN units overlapped with those of the population of IC units with
479 the higher threshold differences (grey shaded region).

480 The neurometric-psychometric comparisons were performed for all CN units, and the
481 results shown in Figure 6C and D, similar to Figures 4C and D. Resampling methods were used

482 to determine differences between psychometric and neurometric parameters in a manner similar
483 to that described for IC units. Figure 6C shows a comparison of psychometric and neurometric
484 thresholds, using the same format as Figure 4C. Consistent with the exemplars shown in Figure 6
485 and panels 6A and B, the entire population fell under the diagonal line of equal thresholds (solid
486 line), and only a small number of CN units had neurometric thresholds that did not differ
487 significantly from psychometric thresholds (p>0.05; open circles, Figure 6C). CN neurometric
488 thresholds were, on average, higher than psychometric thresholds (median threshold difference =
489 19.8 dB), and significantly different from psychometric thresholds (Wilcoxon signed ranksum
490 test, Z=3.41, p= 6.5x10^{-4}). Despite most threshold pairs being significantly different, the
491 psychometric and neurometric thresholds were still correlated (r=0.46, p<0.05), suggesting that
492 even though psychometric and neurometric thresholds were different in magnitude, higher
493 (lower) psychometric thresholds were measured along with higher (lower) CN neurometric
494 thresholds. However, much like the IC data, these were based on the relationship between the
495 thresholds and unit CF; thus the partial correlation between psychometric and neurometric
496 thresholds while using CF as a covariate was not statistically significant. Further, the variance of
497 the CN thresholds (re: psychometric thresholds) were significantly different from the variance of
498 the IC neurometric thresholds (re: psychometric thresholds (Ansari Bradley test, W=4398,
499 W*=2.5685, p = 0.0078).

500 A comparison of the slopes of the psychometric and CN neurometric functions is shown
501 in Figure 6D. In spite of the dichotomy of the exemplars shown in Figure 5, across the
502 population, there was no segregation of type I and type III units slopes and their relationships
503 with the psychometric slope. A larger proportion of CN neurometric slopes were significantly
504 different from the psychometric slope relative to the IC (compare filled circles, Figures 4D and

505 6D). On the average, CN neurometric slopes were shallower than the psychometric slopes
506 (median difference=-0.014/dB); the difference between the neurometric and psychometric slopes
507 for CN units was significantly different from zero (Wilcoxon signed ranksum test, Z=2.91,
508 p=3.61x10^{-3}). The differences between psychometric and neurometric slope in the CN and the IC
509 were significantly different from each other (Wilcoxon rank sum test, Z=2.08, p=0.075),
510 suggesting that the neurometric sensitivity to tone level differences was larger in the IC than in
511 the CN.

512 *Detect probabilities (DP)*

513 Early studies posited that for unit responses to be related to perception, the variability in
514 neuronal responses should be related to behavioral variability on a trial-by-trial basis (Britten et
515 al. 1996; Parker and Newsome 1998). More recently, studies have provided evidence that these
516 relationships reflect interneuronal correlation structure (Liu et al. 2013; Zaidel et al. 2017). In
517 this study the relationship between neuronal and behavioral variability was quantified using the
518 detect probability measure (DP, see Methods; after Britten et al. 1996; Cook and Maunsell 2002;
519 Kang and Maunsell 2012), which provides an estimate of the probability that an ideal observer
520 could predict behavioral accuracy based on spiking activity. Figure 7A shows the DPs for all IC
521 units. About 75% of IC units (n=81/108) showed DP values that were significantly different
522 from 0.5, and thus significant response differences related to behavioral outcome; most of these
523 were units that had DP values greater than 0.5 (black bars; responses that were higher on correct
524 trials relative to incorrect trials), and the rest were units that showed DP values less than 0.5.
525 Significance of each DP was determined by resampling (see Methods), followed by permutation
526 test, after Kang and Maunsell (2012). The median DP value was 0.647, while the mean was 0.62,
527 suggesting that correct trials were correlated with larger total responses in the IC. DP values

528 were calculated for CN units, and their distribution is shown in Figure 7B. The distribution of DP
529 for CN units was centered closer to 0.5 than the corresponding distribution for IC units. Smaller
530 proportions of units showed DP values significantly different than 0.5: some units (n=23, 25.3%)
531 showed DP values greater than chance (increased responses on correct trials, black filled bars),
532 while others (n=14, 15.3%) showed DP values less than 0.5 (corresponding to decreased
533 responses on correct trials relative to incorrect trials, black bars). The median value of DP for CN
534 single units was 0.53, not significantly different than chance (permutation test, $p = 0.11$). The
535 distributions of DPs in the IC and CN were significantly different, as assessed by a 2-sample
536 Kolmogorov-Smirnov test ($p = 0.003$).

537 Many studies have measured CP or DP as a function of time (response duration) to gain
538 insight into the origin of choice related activity in sensory neurons (see Discussion). In this
539 study, DPs were calculated using different time-windows, beginning at tone onset. Figure 7 C-D
540 depicts the mean (+/- SEM) DP across the population in the IC (Figure 7C) and CN (Figure 7D).
541 DPs were concentrated at 0.5 at the beginning of the response, and diverged from chance within
542 the first 75 ms, on average. Some units increased DP over time (black error bands in Figure 7C
543 and D), while others decreased DP over time (white error bands). To more closely inspect this
544 trend, the time required to reach a significant DP was calculated for each neuron exhibiting a
545 significant DP. Most neurons exhibiting a significant DP in the IC (Figure 7E) and CN (Figure
546 7F) reached significance in the first 100 ms. This is apparent in the proportion histograms, whose
547 peak bins occur 50-100 ms. The mean time to significance was 64.9 ms in the IC, and 67.8 ms in
548 the CN. The distributions of time-to-significance values were not significantly different between
549 brain regions (Kolmogorov-Smirnov test, $p = 0.9$).

550 *No trial by trial correlation between subcortical neuronal responses and reaction time*

551 Behavioral reaction times (RTs) decreased as the tone sound pressure level increased
552 (e.g., Green et al. 1966; Dylla et al. 2013). Figure 8 shows the relationship between response
553 magnitudes and RT for CN and IC units. Figures 8A and D shows how RT co-varied with the
554 responses for the exemplar IC unit from Figure 2A and the exemplar CN unit in Figure 6A,
555 respectively. In general, RTs decreased as the response magnitude increased. A linear fit best
556 captured the variability of the data (shown by the black line), and its slope was termed the
557 neurometric RT slope. For most units (IC: 96%; CN: 96%), the neurometric RT slopes were
558 significantly different from zero ($p<0.05$, as assessed by Monte-Carlo methods, see Methods),
559 suggesting a relationship between response magnitude and RT. However, when the variations in
560 RT and response magnitude were compared on a trial-by-trial basis at each sound pressure level,
561 the two parameters were not significantly correlated ($p > 0.05$, examples shown in Figure 8B and
562 8E). Thus the relationship between RT and response magnitude for CN and IC neurons may be
563 an epiphenomenon of the relationship between response magnitude and tone level. Similar
564 results were obtained in analyses of latency. Latencies were longer at lower sound levels (when
565 RTs were longer), and shorter at higher sound levels (when RTs were shorter). A linear fit could
566 account for the relationship between latencies and RTs (similar to figures 8A and C), but there
567 was no significant relationship between RTs and the related neurophysiological latencies on a
568 trial-by-trial basis at each sound level (Figure 8B and 8E). Consistent with these findings,
569 multiple regression between response magnitude (or latency) and reaction time including sound
570 pressure level as a covariate resulted in partial correlations that were not statistically significant
571 ($p>0.05$). The distribution of the neurometric RT slope (Neurometric RTS) for IC and CN single
572 units are shown in Figures 8C and F. All slope values were negative, indicating that RT
573 decreased as IC and CN responses increased for all units in this population, with a median rate of

574 -3.1 ms/spike. The distribution of neurometric RT slopes for CN units (shown in Figure 8F) was
575 not significantly different than that found for IC units (Wilcoxon ranksum test, $p>0.2$).
576 *Pooling analysis*
577 The finding that IC but not CN responses provided accurate estimates of psychometric
578 threshold and slope (Figure 9A) begs the question of whether and how converging inputs to the
579 IC could provide such psychometric-neurometric correlations. Though previous studies have
580 addressed the question of how IC responses emerge from CN inputs (Nelson and Carney 2004;
581 Hewitt and Meddis 1994), none have used CN data from behaving animals to address how
582 psychometric performance can emerge from population responses. To test this idea, two different
583 kinds of pooling analyses of CN neuronal responses were performed (see Methods): uniform
584 pooling, which indiscriminately samples the population under the assumption that any neuron
585 can contribute to detection performance, and selective pooling based on the lower envelope
586 principle, which states that performance reflects the responses of the most sensitive neurons in
587 the population. Figure 9B shows how simulated populations of CN units exhibit progressively
588 lower median threshold as a function of the number of units in the population. These trends were
589 fit with a power-law function to permit interpolation between different population sizes. Uniform
590 pooling resulted in a median threshold trend that equaled the IC, and behavior, at a population
591 size of about 25 neurons, whereas the selective pooling approach resulted in pooled thresholds
592 approximating behavior using about 10 units. Figure 9C shows how uniform pooling impacted
593 the slopes of neurometric functions of small populations. The median slope of the model
594 increased systematically as the population size increased, suggesting that IC slopes and
595 psychometric slopes could be explained by pooling, however, the variability of the slopes was

596 greater than that observed for the IC. Interpretation of these results and necessary caveats are
597 addressed in the Discussion section.

598 **Discussion**:

599 *Neuronal responses and perception*

600 The results presented here are the first direct neurometric-psychometric correlations
601 reported in the subcortical auditory system. These correlations are similar to studies of cortical
602 regions across sensory modalities (auditory: Lemus et al. (2009b); visual: Britten et al. 1992,
603 1996; Cook and Maunsell 2002; Purushothaman and Bradley 2005; Palmer et al. 2007;
604 somatosensory: Hernandez et al. 2000; olfactory: Uchida and Mainen 2003), and results in the
605 subcortical vestibular nucleus (Liu et al. 2013). However, they differ in that subcortical
606 neurometric thresholds in the somatosensory system (Vazquez et al. 2012) and visual system
607 (Jiang et al. 2015) did not match psychometric parameters, but IC responses in this study
608 provided excellent estimates of psychometric threshold and slope.

609 These results also contribute to the understanding of sound detection. The strong match
610 between IC response magnitude and behavioral performance is consistent with other studies
611 showing similarity between behavioral and IC neurophysiological measures (critical bands: Ehret
612 and Merzenich 1985, 1988; Franssen effect: Rajala et al. 2013). However, this does not negate
613 the importance of the cortex for detection (Adams 1986; Heffner and Heffner 1986, 1989, 1990).
614 If the readout of IC information is represented in the cortex, lesions of cortex might disrupt
615 detection. Alternatively, in primates the connections between auditory and motor regions may
616 make the auditory cortex an essential part of the circuit.

617 Beyond providing insight into readout of auditory information, the present results also
618 relate to theories of information readout derived from other sensory systems, namely that

619 behavior is about as sensitive as the average neuron in visual and somatosensory cortex (Britten
620 et al. 1992; Hernandez et al. 2000). This is in contradiction with the lower envelope principle,
621 which states that the behavioral response is best correlated with the most sensitive neurons
622 (visual cortex: Parker and Newsome 1998; auditory cortex: Johnson et al. 2012). The enhanced
623 sensitivity of the IC relative to the CN begs the question of how neuronal sensitivity in the IC
624 arises from its inputs, which was addressed via pooling (Figure 9B and 9C). The pooling results
625 suggest converging CN inputs can provide accurate estimates of threshold and slope, with pooled
626 CN threshold matching the IC and behavior at a population size of about 10 (lower envelope
627 pooling strategy) or 25 (uniform pooling strategy) units. Anatomically, this pooling is an
628 oversimplification because the IC receives, in addition to CN inputs, inputs from the superior
629 olivary complex, the nuclei of the lateral lemniscus, the contralateral IC, thalamus, and from the
630 cortex (Reviewed in Oliver and Huerta (1992); Schreiner and Winer (2005); and Moore et al.
631 (2010)). However, it provides the first demonstration that small populations in the CN can
632 explain behavior using data from behaving animals and lends support to models that invoke CN-
633 IC convergence to explain IC responses and behavior (Nelson and Carney 2004; Hewitt and
634 Meddis 1994). The finding that small populations of CN neurons can explain behavior is
635 consistent with other work in an amplitude-modulation (AM) discrimination paradigm (Mackey
636 et al. 2022), which is interesting compared to previous pooling studies reporting that similar
637 numbers of primary auditory cortical neurons are required to explain AM detection behavior in
638 macaques (Johnson et al. 2012). This may indicate that perceptual sensitivity attributed to
639 auditory cortex may in fact be inherited from population activity in subcortical regions. The
640 pooling results are presented with the caveat that interneuronal correlations impair the decoding

641 of population activity (Moreno Bote et al. 2014), and due to the recording methods here,
642 interneuronal correlations are not available, an issue that is elaborated upon below.
643 *Trial-by-trial correlation between neuronal activity and behavioral performance*
644 The covariation between the neuronal response magnitude and behavioral responses on a
645 trial-by-trial basis (Detect probability; Figure 7) are the first reported significant neuronal
646 correlates of behavioral choice in the subcortical auditory system; and one of the few reports of
647 subcortical choice-related activity in any sensory system (Liu et al. 2013). This contrasts
648 previous studies from Kettner and Thompson (1980, 1985), where correlations between neural
649 and behavioral variability were found only outside of the auditory pathway. This difference
650 could be due to species differences (rabbit vs. primate), or more likely, task differences (classical
651 conditioning vs. operant behavior). The DP values reported here for the IC (median =0.647,
652 mean = 0.62) are comparable with the values of choice probability (CP) in the subcortical
653 vestibular nucleus (mean = 0.61, Liu et al. 2013). Interestingly these values from subcortical
654 stations are higher than those reported in studies of primary auditory cortex (Niwa et al. 2012a)
655 and visual cortical area MT during discrimination (mean = 0.555, Britten et al. 1996), and larger
656 than values for primary visual cortex during detection (mean = 0.52, Palmer et al. 2007). One
657 reason that VN neurons have larger CP values could be due to their direct connections with
658 motor nuclei; another possibility that the authors mention is the strong relationship between
659 noise correlation and signal correlation in VN (Liu et al. 2013). While we did not measure noise
660 correlations, one study found no significant noise correlations in the IC of anesthetized guinea
661 pigs in response to speech sounds (Garcia Lazaro et al. 2013). There are currently no
662 descriptions of noise correlation values in CN or IC in awake animals that could compare with
663 this study or highlight the generality of the findings by Liu et al. (2013) for other sensory

664 systems. The emergence of significant choice probabilities in early sensory areas may be due to
665 input from higher order regions (Nienborg and Cumming 2009; Zaidel et al. 2017), and may
666 reflect other non-circuit related factors, such as cognitive state, or the nature of the task
667 (Nienborg et al. 2012). Consistent with this, our group and others have reported task-related
668 modulation of activity in the IC (Rocchi and Ramachandran 2020; Ryan et al. 1984; Shaheen et
669 al. 2021). Another possibility is that response variability in ANF response may introduce a small,
670 statistically non-significant bias between correct and incorrect responses; convergence, such as
671 those in the CN (e.g., Wang and Delgutte 2013), and those between CN and IC, may induce
672 correlated noise that magnifies these effects to reach statistical significance at the IC. Regardless
673 of the underlying circuitry, the evolution of DP over time in the present data suggests it is a rapid
674 process (Figure 7E).

675 A population of IC units showed significant DP values < 0.5 (their responses on correct
676 trials were lower compared to incorrect trials; Figure 7A). Similar findings have been reported in
677 the visual system: Bosking and Maunsell (2011) report that the DP of some visual neurons
678 (specifically, whose tuning matched the stimulus parameters at the onset of the task) were
679 significantly higher than 0.5; neurons with opposite tuning had DP less than chance. Neurons
680 with DP < 0.5 may perform similar functions as those with DP>0.5. Additionally, the speculation
681 of push-pull action of the populations with DPs above and below 0.5 are intriguing, though the
682 segregating factor was not the monotonicity. Some IC projections to the thalamus are inhibitory
683 (Winer et al. 1996; Peruzzi et al. 1997; Mellott et al. 2014, 2019). The inhibitory and excitatory
684 output neurons could represent the two disparate populations with DP values above and below
685 0.5. Such convergence could increase the thalamic response contrast between correct and
686 incorrect responses, and may relate to performance monitoring and reward expectation.

The relative paucity of strong correlations between fluctuations in the responses of CN neurons (the first central synaptic station in the auditory system) and behavioral variability is consistent with suggestions of early anatomical work that auditory functions in nonhuman primates are more encephalized (e.g., Adams 1986). The reduced correlations may be only for response magnitude, and not for responses in general; temporal aspects of CN response encoded behavior better than magnitudes (Gai and Carney 2006; Gai et al. 2007). While Gai et al. compared neuronal responses and behavioral responses obtained at different times and in a different species, the possibility of a correlation between behavior and the temporal aspects of CN and IC responses is currently being explored with this and other data sets (Ramachandran, 2018), as well as its implications on circuitry.

These results represent an important step in understanding how subcortical activity relates to auditory perception, how choice-related activity is reflected along the auditory pathway, and provide a baseline for future studies of hearing loss.

References:

Adams JC (1986) Neuronal morphology in the human cochlear nucleus. Arch Otolaryngol Head Neck Surg 112:1253-1261.

Barlow HB, Levick WR, Yoon M (1971) Responses to single quanta of light in retinal ganglion cells of the cat. Vision Res Suppl 3:87-101.

Behrens, D., & Klump, G. M. (2016). Comparison of mouse minimum audible angle determined in prepulse inhibition and operant conditioning procedures. Hearing research, 333, 167-178.

Bohlen P, Dylla M, Timms C, Ramachandran R (2014) Detection of modulated tones in modulated noise by non-human primates. J Assoc Res Otolaryngol 15:801-821.

711 Bosking WH, Maunsell JH (2011) Effects of stimulus direction on the correlation between
712 behavior and single units in area MT during a motion detection task. J Neurosci
713 31(22):8230-8.
714 Britten KH, Newsome WT, Shadlen MN, Celebrini S, Movshon JA (1996) A relationship
715 between behavioral choice and the visual responses of neurons in macaque MT. Vis
716 Neurosci 13:87-100.
717 Britten KH, Shadlen MN, Newsome WT, Movshon JA (1992) The analysis of visual motion: a
718 comparison of neuronal and psychophysical performance. J Neurosci 12:4745-4765.
719 Cant NB (1992) The cochlear nucleus: neuronal types and their synaptic organization. In: The
720 mammalian auditory pathway: Neuroanatomy (Webster DB, Popper AN, Fay RR, eds),
721 pp 66-116. New York, NY: Springer-Verlag.
722 Chase SM, Young ED (2005) Limited segregation of different types of sound localization
723 information among classes of units in the inferior colliculus. J Neurosci 25:7575-7585.
724 Christison-Lagay, KL, Bennur, S, & Cohen, YE. (2017). Contribution of spiking activity in the
725 primary auditory cortex to detection in noise. Journal of Neurophysiology, 118(6), 3118-
726 3131.
727 Cohen MR, Newsome WT (2009) Estimates of the contribution of single neurons to perception
728 depend on timescale and noise correlation. J Neurosci 29:6635-6648.
729 Cook EP, Maunsell JH (2002) Dynamics of neuronal responses in macaque MT and VIP during
730 motion detection. Nat Neurosci. 5(10):985-94.
731 Davis KA (2002) Evidence of a functionally segregated pathway from dorsal cochlear nucleus to
732 inferior colliculus. J Neurophysiol 87:1824-1835.
733 Delgutte, B. (1996). Physiological models for basic auditory percepts. In *Auditory*

computation (pp. 157-220). Springer, New York, NY.

Ditterich, J., Mazurek, M. E., & Shadlen, M. N. (2003). Microstimulation of visual cortex affects the speed of perceptual decisions. Nature neuroscience, 6(8), 891-898.

Dylla M, Hrnicek A, Rice C, Ramachandran R (2013) Detection of tones and their modification by noise in nonhuman primates. J Assoc Res Otolaryngol 14:547-560.

Ehret G, Merzenich MM (1985) Auditory midbrain responses parallel spectral integration phenomena. Science. 227(4691):1245-7.

Ehret G, Merzenich MM (1988) Complex sound analysis (frequency resolution, filtering and spectral integration) by single units of the inferior colliculus of the cat. Brain Res. 472(2):139-63.

Evans EF, Nelson PG (1973) The responses of single neurones in the cochlear nucleus of the cat as a function of their location and the anaesthetic state. Exp Brain Res 17:402-427.

Francis, NA, Winkowski, DE, Sheikhattar, A, Armengol, K, Babadi, B, & Kanold, PO (2018). Small networks encode decision-making in primary auditory cortex. Neuron, 97(4), 885-897.

Gai Y, Carney LH (2006) Temporal measures and neural strategies for detection of tones in noise based on responses in anteroventral cochlear nucleus. J Neurophysiol 96:2451-2464.

Gai Y, Carney LH, Abrams KS, Idrobo F, Harrison JM, Gilkey RH (2007) Detection of tones in reproducible noise maskers by rabbits and comparison to detection by humans. J Assoc Res Otolaryngol 8:522-538.

Garcia-Lazaro JA, Belliveau LA, Lesica NA (2013) Independent population coding of speech with sub-millisecond precision. J Neurosci 33(49):19362-72.

Gerken, G. M. (1970). Electrical stimulation of the subcortical auditory system in behaving cat. Brain Research, 17(3), 483–497. https://doi.org/https://doi.org/10.1016/0006-8993(70)90255-6

Goldberg JM, Brown PB (1969) Response of binaural neurons of dog superior olivary complex to dichotic tonal stimuli: some physiological mechanisms of sound localization. J Neurophysiol 32:613-636.

Green DM, Swets JA (1966) Signal detection theory and psychophysics. Huntingdon, NY: Krieger.

Heffner HE, Heffner RS (1986) Hearing loss in Japanese macaques following bilateral auditory cortex lesions. J Neurophysiol 55:256-271.

Heffner HE, Heffner RS (1989) Unilateral auditory cortex ablation in macaques results in a contralateral hearing loss. J Neurophysiol 62:789-801.

Heffner HE, Heffner RS (1990) Effect of bilateral auditory cortex lesions on absolute thresholds in Japanese macaques. J Neurophysiol 64:191-205.

Hernandez A, Zainos A, Romo R (2000) Neuronal correlates of sensory discrimination in the somatosensory cortex. Proc Natl Acad Sci U S A 97:6191-6196.

Hewitt, M. J., & Meddis, R. (1994). A computer model of amplitude-modulation sensitivity of single units in the inferior colliculus. *The Journal of the Acoustical Society of America*, *95*(4), 2145-2159.

Jiang Y, Yampolsky D, Purushothaman G, Casagrande VA (2015) Perceptual decision related activity in the lateral geniculate nucleus. J Neurophysiol 114(1):717-735.

Johnson, J. S., Yin, P., O'Connor, K. N., & Sutter, M. L. (2012). Ability of primary auditory cortical neurons to detect amplitude modulation with rate and temporal codes:

780 neurometric analysis. Journal of neurophysiology, 107(12), 3325-3341.
781 Kang, I., & Maunsell, J. H. (2012). Potential confounds in estimating trial-to-trial correlations
782 between neuronal response and behavior using choice probabilities. Journal of
783 neurophysiology, 108(12), 3403-3415.
784 Kettner RE, Shannon RV, Nguyen TM, Thompson RF (1980) Simultaneous behavioral and
785 neural (cochlear nucleus) measurement during signal detection in the rabbit. Percept
786 Psychophys 28:504-513.
787 Kettner RE, Thompson RF (1982) Auditory signal detection and decision processes in the
788 nervous system. J Comp Physiol Psychol 96:328-331.
789 Kettner RE, Thompson RF (1985) Cochlear nucleus, inferior colliculus, and medial geniculate
790 responses during the behavioral detection of threshold-level auditory stimuli in the rabbit.
791 J Acoust Soc Am 77:2111-2127.
792 Kiang NYS, Watanabe T, Thomas EC, Clarke LF (1965) Discharge pattern of single fibers inthe
793 cat's auditory nerve. M.I.T. Press.
794 Kuwada S, Stanford TR, Batra R (1987) Interaural phase-sensitive units in the inferior colliculus
795 of the unanesthetized rabbit: effects of changing frequency. J Neurophysiol 57:1338-
796 1360.
797 Lonsbury-Martin, B. L., Martin, G. K., & Bohne, B. A. (1987). Repeated TTS exposures in
798 monkeys: Alterations in hearing, cochlear structure, and single-unit thresholds. *The*
799 *Journal of the Acoustical Society of America*, *81*(5), 1507-1518.
800 Lee JH, Russ BE, Orr LE, Cohen YE (2009) Prefrontal activity predicts monkeys' decisions
801 during an auditory category task. Front Integr Neurosci 3:16.
802 Lemus L, Hernandez A, Romo R (2009) Neural encoding of auditory discrimination in ventral

803 premotor cortex. Proc Natl Acad Sci U S A 106:14640-14645.
804 Lemus L, Hernandez A, Romo R (2009) Neural codes for perceptual discrimination of acoustic
805 flutter in the primate auditory cortex. Proc Natl Acad Sci U S A 106:9471-9476.
806 Lisberger SG, Pavelko TA, Bronte-Stewart HM, Stone LS (1994) Neural basis for motor
807 learning in the vestibuloocular reflex of primates. II. Changes in the responses of
808 horizontal gaze velocity Purkinje cells in the cerebellar flocculus and ventral
809 paraflocculus. J Neurophysiol 72:954-973.
810 Liu S, Gu Y, DeAngelis GC, Angelaki DE (2013) Choice-related activity and correlated noise in
811 subcortical vestibular neurons. Nat Neurosci 16:89-97.
812 Mackey, C. A., Hauser, S., Schoenhaut, A. M., Temghare, N., & Ramachandran, R. (2022).
813 Psychometric and subcortical neurometric measures of temporal discrimination in rhesus
814 macaques. *bioRxiv*.
815 May BJ, Huang AY (1997) Spectral cues for sound localization in cats: a model for discharge
816 rate representations in the auditory nerve. J Acoust Soc Am 101:2705-2719.
817 Mellott, J. G., Foster, N. L., Ohl, A. P., & Schofield, B. R. (2014). Excitatory and inhibitory
818 projections in parallel pathways from the inferior colliculus to the auditory
819 thalamus. Front Neuroanat, 8, 124.
820 Mellott, J. G., Beebe, N. L., & Schofield, B. R. (2019). Bilateral projections to the thalamus from
821 individual neurons in the inferior colliculus. J Comp Neurol, 527(6), 1118-1126.
822 Merzenich MM, Reid MD (1974) Representation of the cochlea within the inferior colliculus of
823 the cat. Brain Res 77:397-415.
824 Moerel, M., De Martino, F., Uğurbil, K., Yacoub, E., & Formisano, E. (2015). Processing of
825 frequency and location in human subcortical auditory structures. Scientific reports, 5(1),

1-15.

Moore, D. R., Fuchs, P. A., Rees, A., Palmer, A. R., & Plack, C. J. (Eds.). (2010). The Oxford handbook of auditory science: The auditory brain (Vol. 2). Oxford University Press. Pages 9-43.

Moore JK (1980) The primate cochlear nuclei: loss of lamination as a phylogenetic process. J Comp Neurol 193:609-629.

Moore JK, Osen KK (1979) The cochlear nuclei in man. Am J Anat 154:393-418.

Moreno-Bote R, Beck J, Kanitscheider I, Pitkow X, Latham P, Pouget A (2014) Information limiting correlations. Nat Neurosci 17:1410-1417.

Morest DK, Oliver DL (1984) The neuronal architecture of the inferior colliculus in the cat: defining the functional anatomy of the auditory midbrain. J Comp Neurol 222:209-236.

Murasugi, C. M., Salzman, C. D., & Newsome, W. T. (1993). Microstimulation in visual area MT: effects of varying pulse amplitude and frequency. Journal of Neuroscience, 13(4), 1719-1729.

Nelken I, Young ED (1994) Two separate inhibitory mechanisms shape the responses of dorsal cochlear nucleus type IV units to narrowband and wideband stimuli. J Neurophysiol 71:2446-2462.

Nelson PC, Smith ZM, Young ED (2009) Wide-dynamic-range forward suppression in marmoset inferior colliculus neurons is generated centrally and accounts for perceptual masking. J Neurosci 29:2553-2562.

Nelson, P. C., & Carney, L. H. (2004). A phenomenological model of peripheral and central neural responses to amplitude-modulated tones. *The Journal of the Acoustical Society of America*, *116*(4), 2173-2186.

849 Nienborg H, Cohen MR, Cumming BG (2012) Decision-related activity in sensory neurons:
850 correlations among neurons and with behavior. Annu Rev Neurosci 35:463-483.
851 Nienborg H, Cumming BG (2009) Decision-related activity in sensory neurons reflects more
852 than a neuron's causal effect. Nature 459:89-92.
853 Niwa M, Johnson JS, O'Connor KN, Sutter ML Active engagement improves primary auditory
854 cortical neurons' ability to discriminate temporal modulation. J Neurosci 32:9323-9334.
855 Niwa M, Johnson JS, O'Connor KN, Sutter ML (2012) Active engagement improves primary
856 auditory cortical neurons' ability to discriminate temporal modulation. J Neurosci
857 32:9323-9334.
858 Niwa M, Johnson JS, O'Connor KN, Sutter ML (2012) Activity related to perceptual judgment
859 and action in primary auditory cortex. J Neurosci 32:3193-3210.
860 Oliver DL, Huerta MF (1992) Inferior and superior colliculi. In: The mammalian auditory
861 pathway: Neuroanatomy (Webster DB, Popper AN, Fay RR, eds), pp 168-221. New
862 York, NY: Springer-Verlag.
863 Palmer C, Cheng SY, Seidemann E (2007) Linking neuronal and behavioral performance in a
864 reaction-time visual detection task. J Neurosci 27:8122-8137.
865 Parker AJ, Newsome WT (1998) Sense and the single neuron: probing the physiology of
866 perception. Annu Rev Neurosci 21:227-277.
867 Peruzzi D, Bartlett E, Smith PH, Oliver DL (1997) A monosynaptic GABAergic input from the
868 inferior colliculus to the medial geniculate body in rat. J Neurosci 17:3766-3777.
869 Pfingst BE, Hienz R, Kimm J, Miller J (1975) Reaction-time procedure for measurement of
870 hearing. I. Suprathreshold functions. J Acoust Soc Am 57:421-430.
871 Pitkow X, Liu S, Angelaki DE, DeAngelis GC, Pouget A (2015) How Can Single Sensory

Neurons Predict Behavior? Neuron 87(2):411-423.

Populin LC (2005) Anesthetics change the excitation/inhibition balance that governs sensory processing in the cat superior colliculus. J Neurosci 25:5903-5914.

Purushothaman G, Bradley DC (2005) Neural population code for fine perceptual decisions in area MT. Nat Neurosci 8:99-106.

Rajala AZ1, Yan Y, Dent ML, Populin LC (2013) The inferior colliculus encodes the Franssen auditory spatial illusion. Eur J Neurosci 38(7): 3056-3070.

Ramachandran R, Davis KA, May BJ (1999) Single-unit responses in the inferior colliculus of decerebrate cats. I. Classification based on frequency response maps. J Neurophysiol 82:152-163.

Ramachandran, R. (2018). Subcortical neural correlates of behavior in the auditory system. The Journal of the Acoustical Society of America, 144(3), 1899-1899.

Reiss LA, Ramachandran R, May BJ (2011) Effects of signal level and background noise on spectral representations in the auditory nerve of the domestic cat. J Assoc Res Otolaryngol 12:71-88.

Rhode, W. S., Roth, G. L., & Recio-Spinoso, A. (2010). Response properties of cochlear nucleus neurons in monkeys. Hearing research, 259(1-2), 1-15.

Rocchi, F., & Ramachandran, R. (2020). Foreground stimuli and task engagement enhance neuronal adaptation to background noise in the inferior colliculus of macaques. Journal of Neurophysiology, 124(5), 1315-1326.

Romo R, Hernandez A, Zainos A, Lemus L, Brody CD (2002) Neuronal correlates of decision-making in secondary somatosensory cortex. Nat Neurosci 5:1217-1225.

Rowland BA, Quessy S, Stanford TR, Stein BE (2007) Multisensory integration shortens

physiological response latencies. J Neurosci 27:5879-5884.

Ryan AF, Miller JM, Pfingst BE, Martin GK (1984) Effects of reaction time performance on single-unit activity in the central auditory pathway of the rhesus macaque. J Neurosci 4:298-308.

Salzman CD, Murasugi CM, Britten KH, Newsome WT (1992) Microstimulation in visual area MT: effects on direction discrimination performance. J Neurosci 12:2331-2355.

Schreiner, C. E., & Winer, J. A. (2005). The inferior colliculus. Springer Science+ Business Media, Incorporated. 115-180.

Shaheen, L. A., Slee, S. J., & David, S. V. (2021). Task engagement improves neural discriminability in the auditory midbrain of the marmoset monkey. Journal of Neuroscience, 41(2), 284-297.

Shofner WP, Young ED (1985) Excitatory/inhibitory response types in the cochlear nucleus: relationships to discharge patterns and responses to electrical stimulation of the auditory nerve. J Neurophysiol 54:917-939.

Siebert WM (1965) Some implications of the stochastic behavior of primary auditory neurons. Kybernetik 2:206-215.

Spirou GA, Young ED (1991) Organization of dorsal cochlear nucleus type IV unit response maps and their relationship to activation by bandlimited noise. J Neurophysiol 66:1750-1768.

Stebbins WC, Green S, Miller FL (1966) Auditory sensitivity of the monkey. Science 153:1646-1647.

Tolhurst DJ, Movshon JA, Dean AF (1983) The statistical reliability of signals in single neurons in cat and monkey visual cortex. Vision Res 23:775-785.

Uchida N, Mainen ZF (2003) Speed and accuracy of olfactory discrimination in the rat. Nat Neurosci 6:1224-1229.

Vazquez Y, Zainos A, Alvarez M, Salinas E, Romo R (2012) Neural coding and perceptual detection in the primate somatosensory thalamus. Proc Natl Acad Sci U S A 109:15006-15011.

Wang GI, Delgutte B (2013) Sensitivity of cochlear nucleus neurons to spatio-temporal changes in auditory nerve activity. J Neurophysiol 108:3172-3195.

Wang, Y., Abrams, K. S., Carney, L. H., & Henry, K. S. (2021). Midbrain-level neural correlates of behavioral tone-in-noise detection: dependence on energy and envelope cues. Journal of Neuroscience, 41(34), 7206-7223.

Weedman DL, Ryugo DK (1996) Projections from auditory cortex to the cochlear nucleus in rats: synapses on granule cell dendrites. J Comp Neurol 371:311-324.

Weedman DL, Ryugo DK (1996) Pyramidal cells in primary auditory cortex project to cochlear nucleus in rat. Brain Res 706:97-102.

Winer JA (2006) Decoding the auditory corticofugal systems. Hear Res 212:1-8.

Winer JA, Saint Marie RL, Larue DT, Oliver DL (1996) GABAergic feedforward projections from the inferior colliculus to the medial geniculate body. Proc Natl Acad Sci U S A 93:8005-8010.

Winer JA, Chernock ML, Larue DT, Cheung SW (2002) Descending projections to the inferior colliculus from the posterior thalamus and the auditory cortex in rat, cat, and monkey. Hear Res. 168: 181-195.

Yang L, Pollak GD, Resler C (1992) GABAergic circuits sharpen tuning curves and modify response properties in the mustache bat inferior colliculus. J Neurophysiol 68:1760-1774.

941 Young ED, Brownell WE (1976) Responses to tones and noise of single cells in dorsal cochlear
942 nucleus of unanesthetized cats. J Neurophysiol 39:282-300.
943 Young ED, Sachs MB (1979) Representation of steady-state vowels in the temporal aspects of
944 the discharge patterns of populations of auditory-nerve fibers. J Acoust Soc Am 66:1381-
945 1403.
946 Young ED, Sachs MB (2008) Auditory nerve inputs to cochlear nucleus neurons studied with
947 cross-correlation. Neuroscience 154:127-138.
948 Young ED, Spirou GA, Rice JJ, Voigt HF (1992) Neural organization and responses to complex
949 stimuli in the dorsal cochlear nucleus. Philos Trans R Soc Lond B Biol Sci 336:407-413.
950 Zaidel, A., DeAngelis, G. C., & Angelaki, D. E. (2017). Decoupled choice-driven and stimulus-
951 related activity in parietal neurons may be misrepresented by choice probabilities. Nature
952 Communications, 8(1), 1-13.
953
954

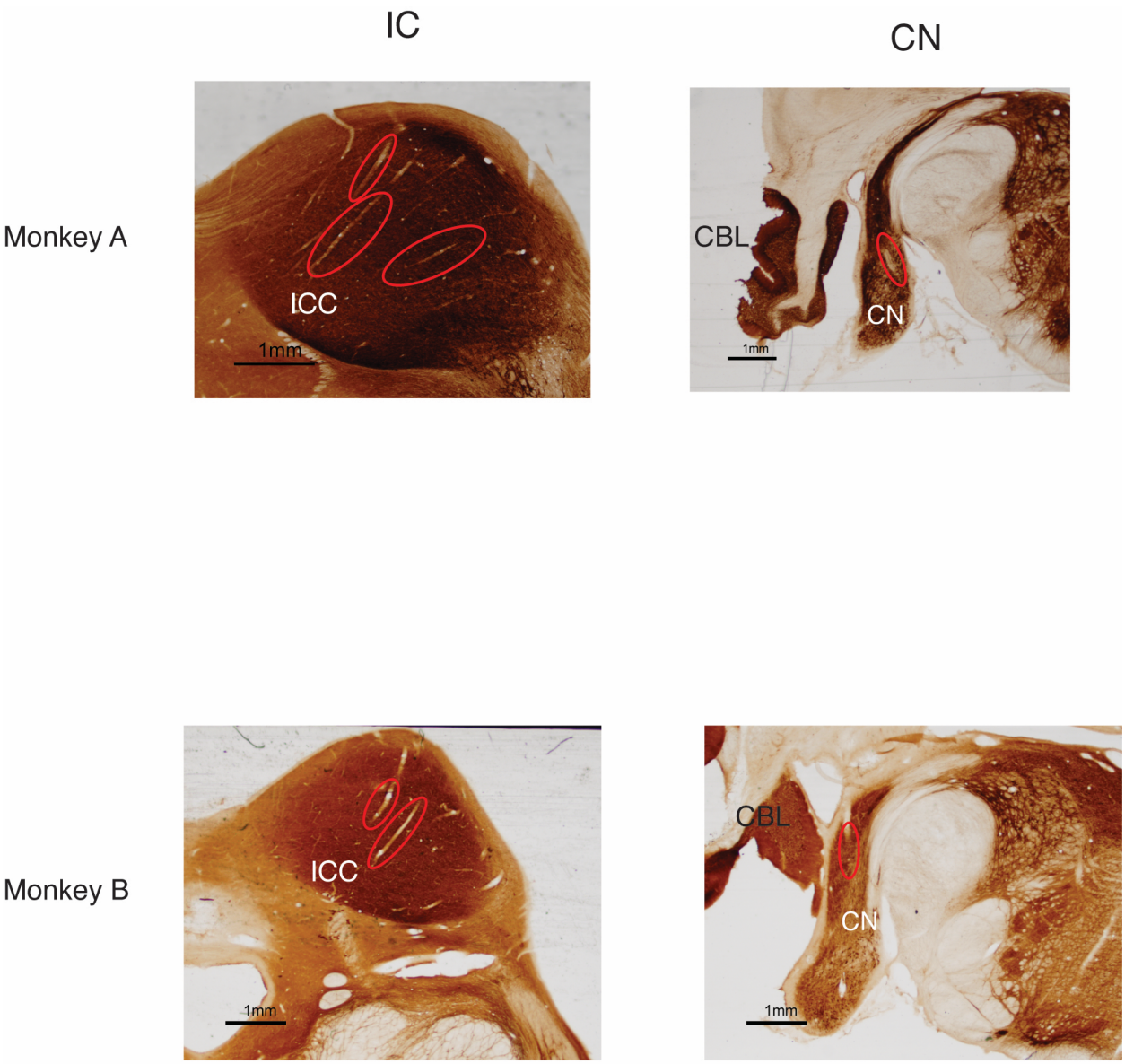

FIGURE 1

Figure 1. Histological sections from two monkeys**.** Examples of coronal sections through the CN and IC. Sections are shown from the brains of two monkeys (Top: monkey A, bottom: monkey B). The columns show sections from the IC (left) and the CN (right). Red ovals outline the electrode tracks at that location. Scale bar (1mm) is shown in each panel.

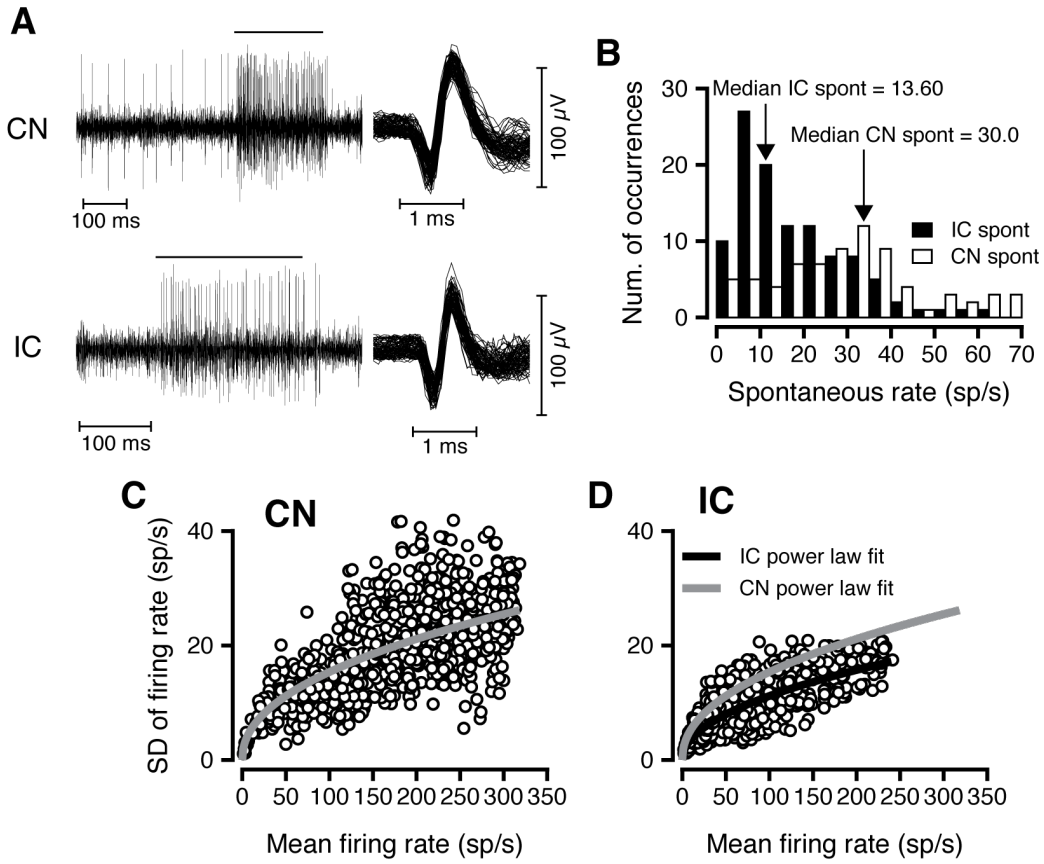

Figure 2. Response statistics in the CN and IC. A. Examples of spike trains and spike snippets. Left: Spike train in one single trial around CF tone presentation is shown for an exemplar IC unit (top), and CN unit (bottom). The duration of stimulus presentation is shown by the horizontal line, and results in greater frequency of spike occurrence in both spike trains. Right: Spike snippets from the IC and CN spike trains. B. Distribution of firing rate in the absence of tones (spontaneous rates) in the CN (open bars) and IC (filled bars). The spontaneous rates were calculated from the spike counts on catch trials (see Methods). C. Relationship between the standard deviation (SD) and mean of the firing rates for CN units. The thick grey line represents the best power law fit to the data ($y=1.85*x^{0.47}$). D. Relationship between mean and standard deviation of firing rates for IC units. The black line represents the best power law fit to the IC

data ($y=0.85*x^{0.46}$). The grey line is the power law fit for CN units, shown for ease of comparison.

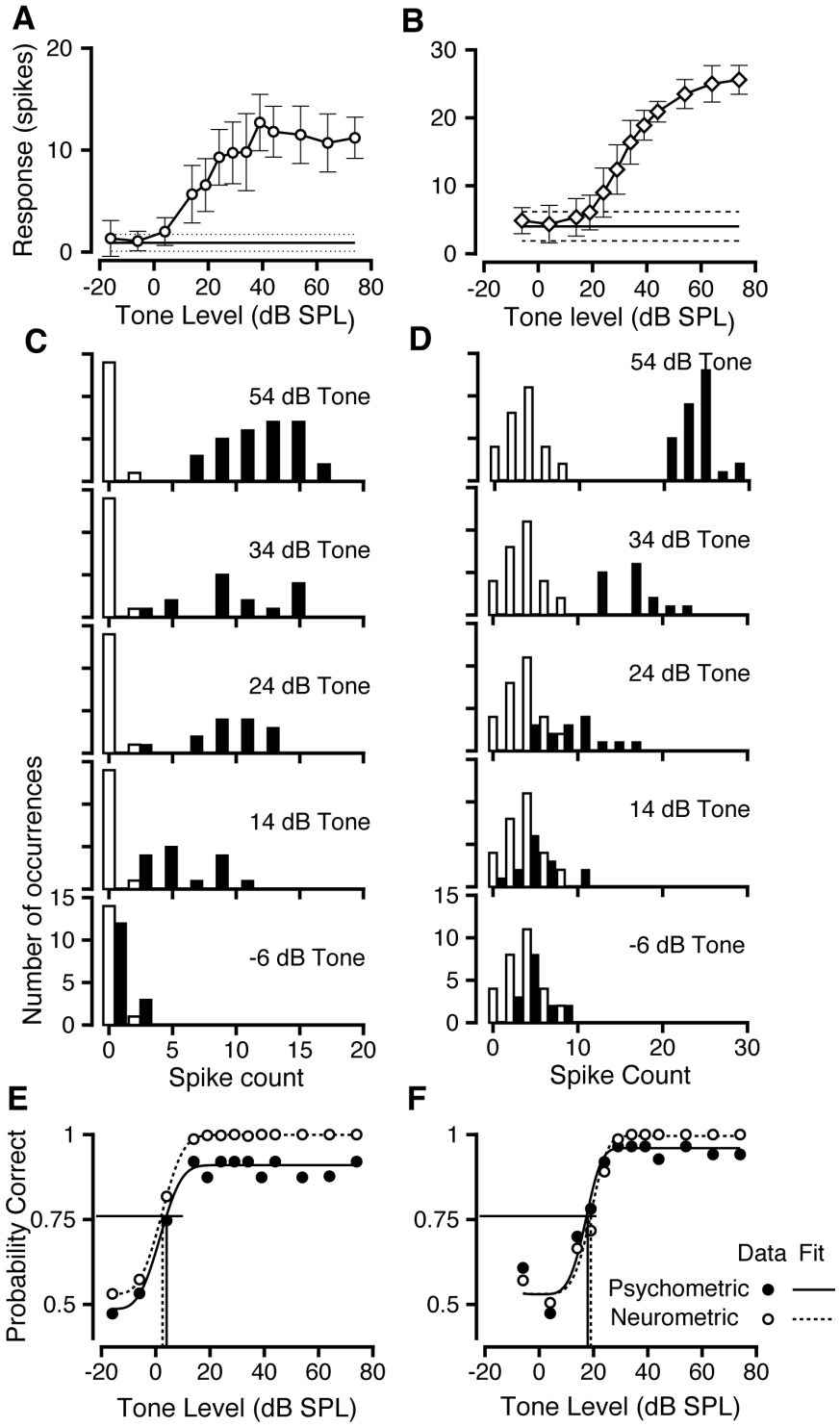

Figure 3. Responses of representative type V (CF=2.2 kHz) and type I units (CF=25.6 kHz) in the IC of the behaving primate to tones at CF as a function of sound pressure level, and ROC

analysis. A, B. Responses (spike count) to a tone at CF as a function of sound pressure level for the type V (A), and type I unit (B). Error bars represent standard deviation of the trial-by-trial spike count. Spontaneous activity is shown as a horizontal line (the range, shown by dashed lines, represents ± 1 standard deviation), and was computed from the spike counts evoked on catch trials. C, D. Distributions of evoked spike counts on catch trials (white bars) and signal trials (filled bars) at various sound pressure levels indicated for the exemplar type V (C) and type I unit (D). E, F. Neurometric functions (open circles) based on the response distributions in panels C and D respectively, plotted along with the psychometric function (filled circles) obtained simultaneously. Solid and dashed lines represent Weibull cdfs fit to the psychometric (solid)) and the neurometric functions (dashed). Solid and dashed vertical lines show psychometric and neurometric thresholds, respectively.

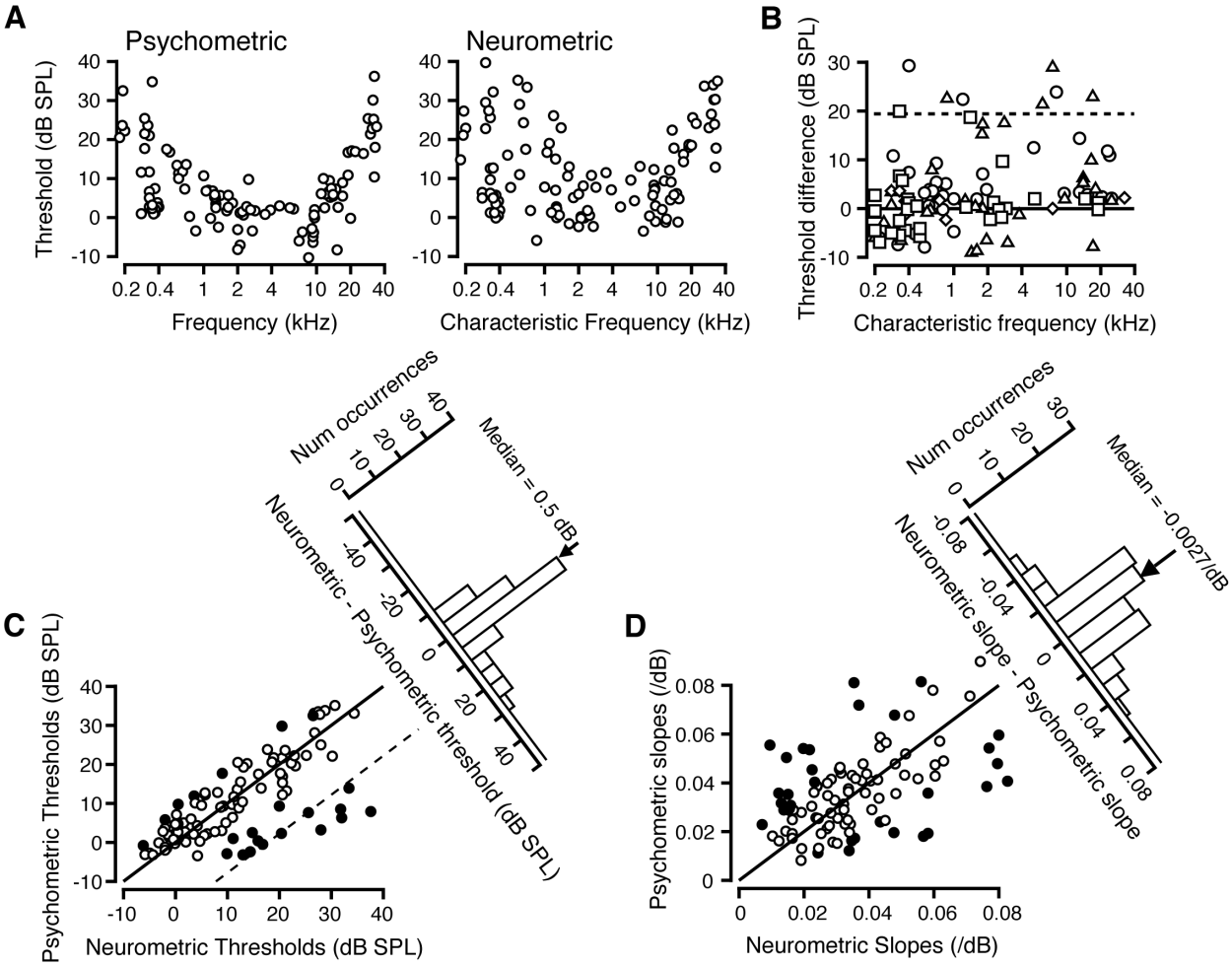

Figure 4. Comparison of psychometric and neurometric parameters in the IC. A. Plot of psychometric thresholds (left) and neurometric thresholds (right) in relation to unit CF. Each circle represents the data obtained while recording the responses of one single unit tuned to the behavioral target tone frequency. B. The difference between psychometric and neurometric threshold is plotted against the CF of the unit. Various symbols represent data from different monkeys. C. Comparison of psychometric and neurometric thresholds. Each symbol represents neurometric threshold from one unit, and the psychometric threshold obtained simultaneously. Filled symbols indicate psychometric and neurometric thresholds significantly different from each other. A histogram of the threshold differences (neurometric – psychometric threshold) is

1003 shown perpendicular to the diagonal. D. Comparison of psychometric and neurometric slopes.

1004 The format is the same as in Figure 4C. The slope difference histogram is shown perpendicular

1005 to the diagonal.

1006

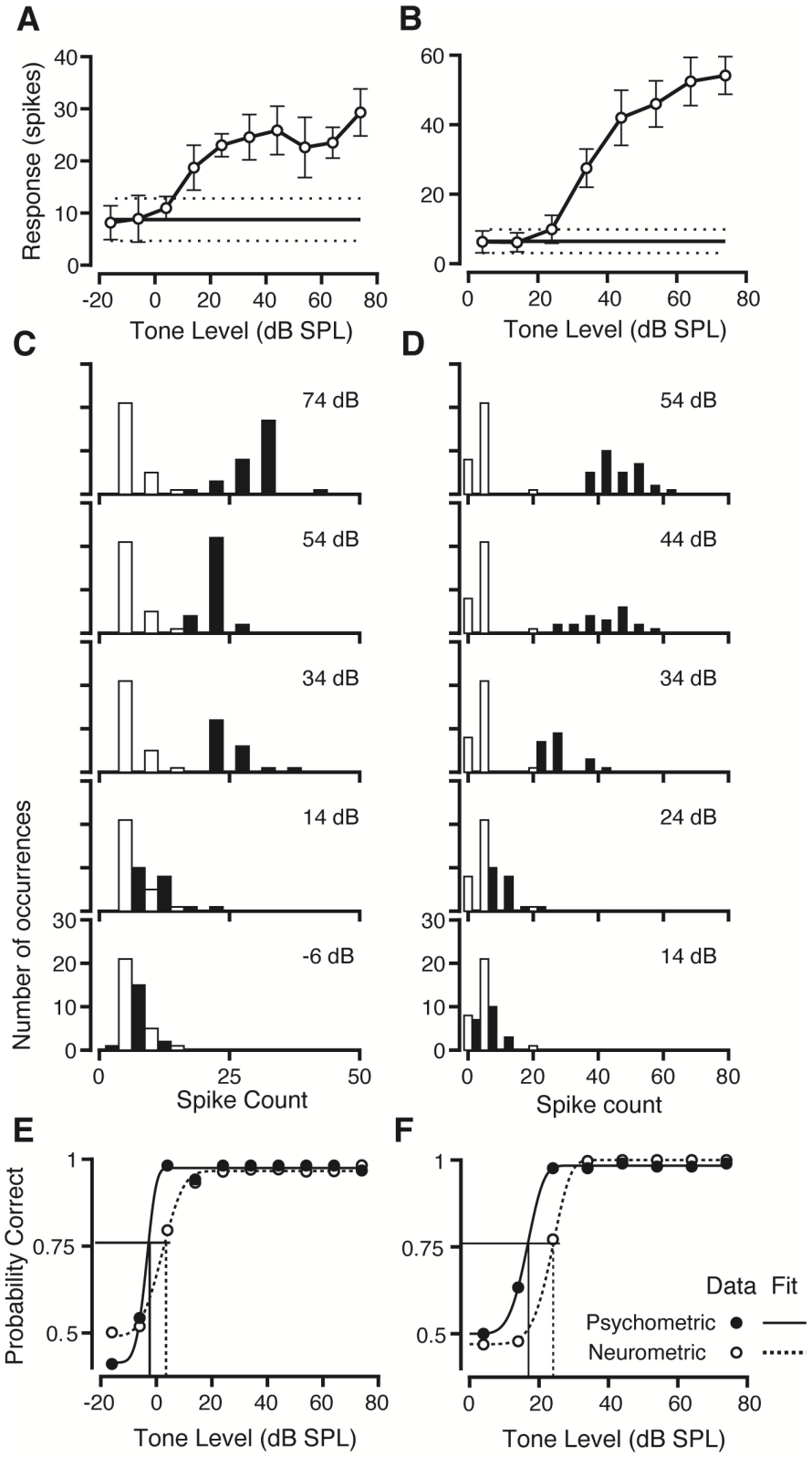
A
B
Response (spikes)
Tone Level (dB SPL)
Tone Level (dB SPL)
C
D
74 dB
54 dB
34 dB
14 dB
-6 dB
54 dB
44 dB
34 dB
24 dB
14 dB
Number of occurrences
Spike Count
Spike count
E
F
Probability Correct
Tone Level (dB SPL)
Tone Level (dB SPL)
Data Fit
Psychometric
Neurometric

1007

1008 **Figure 5**. Responses of units in the CN to tones at CF as a function of sound pressure level, and
1009 results of ROC analysis for type I (CF=2.4 kHz) and type III (CF = 32 kHz) units. The format is
1010 the same as Figure 3. A, B. Responses (spike count) as a function of tone sound pressure level
1011 for a CN type I (A), and CN type III unit (B). C, D. Distribution of evoked spike counts on catch
1012 trials (unfilled bars) and signal trials (filled bars) at the indicated tone sound pressure levels for
1013 the CN type I (C) and the CN type III units (D). E, F. Neurometric functions based on the
1014 distribution of responses in panels C and D (open circles), plotted along with the psychometric
1015 functions obtained simultaneously (filled circles) for the CN type I unit (E) and CN type III unit
1016 (F). Weibull cdf fits for the neurometric (dashed) and psychometric functions (solid) are also
1017 shown. Vertical lines show psychometric (solid) and neurometric thresholds (dashed).

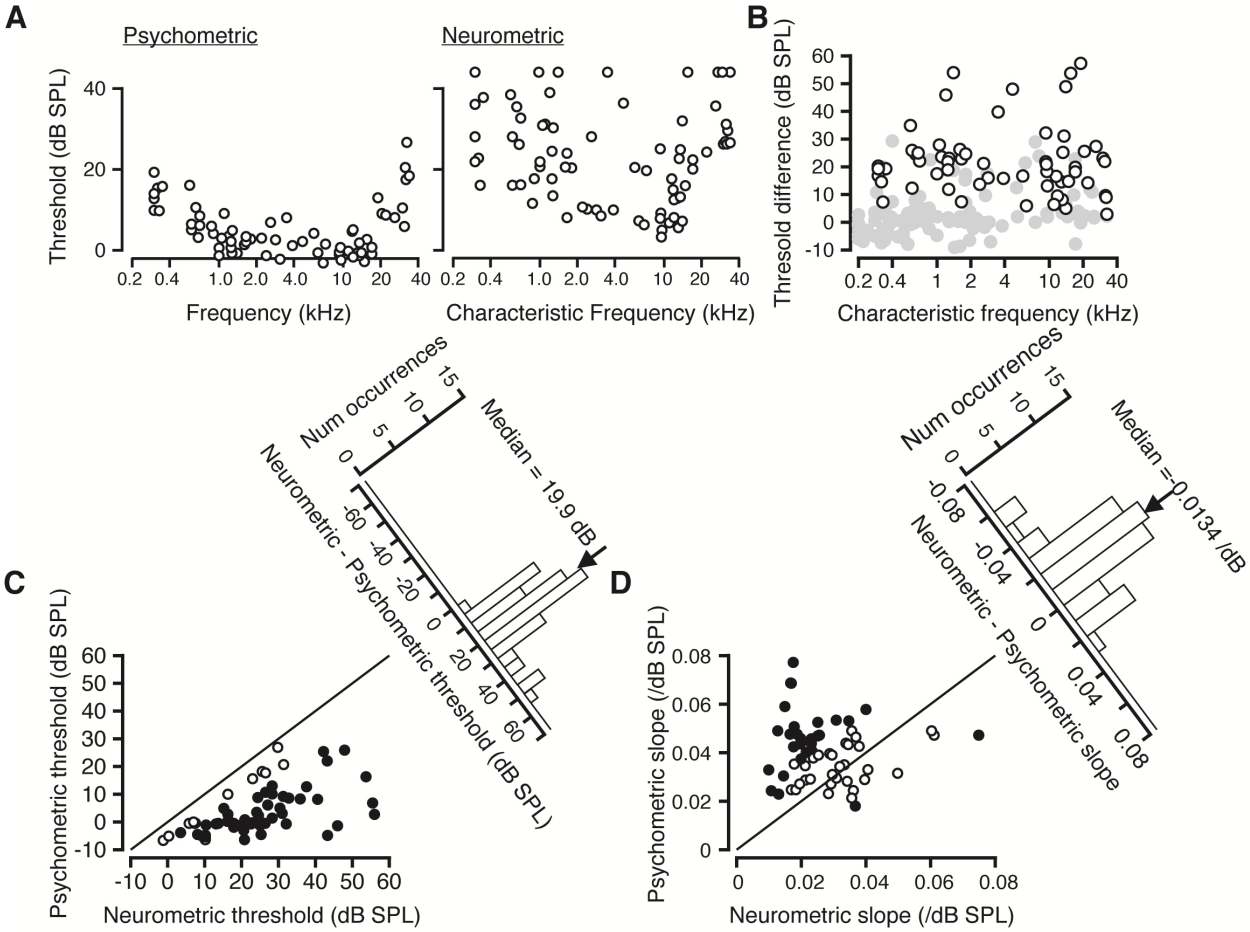

Figure 6. Comparison of psychometric and CN neurometric parameters. Figure uses the same format as Figure 4 and Figure 5B. A. Left, psychometric thresholds plotted against tone frequency. Right, CN neurometric thresholds calculated from responses obtained simultaneously with behavior. Some units have neurometric thresholds higher than 40 dB SPL, and these are shown in a line above the ordinate axis. B. Threshold differences (psychometric – neurometric) vs. the CF of CN units. Format is the same as Figure 4B. IC data (Figure 4B) is shown in grey for comparison. C. Comparison of psychometric and neurometric thresholds of CN single units, and a threshold difference histogram, using the same format as Figure 4A. D. Comparison of psychometric and neurometric slopes, and a slope difference histogram, in the same format as Figure 4C. E. Histogram of DP; format of figure is the same as Figure 5B. Black and grey filled

1029 bars represent units with DP values significantly different higher than and lower than 0.5,

1030 respectively.

1031

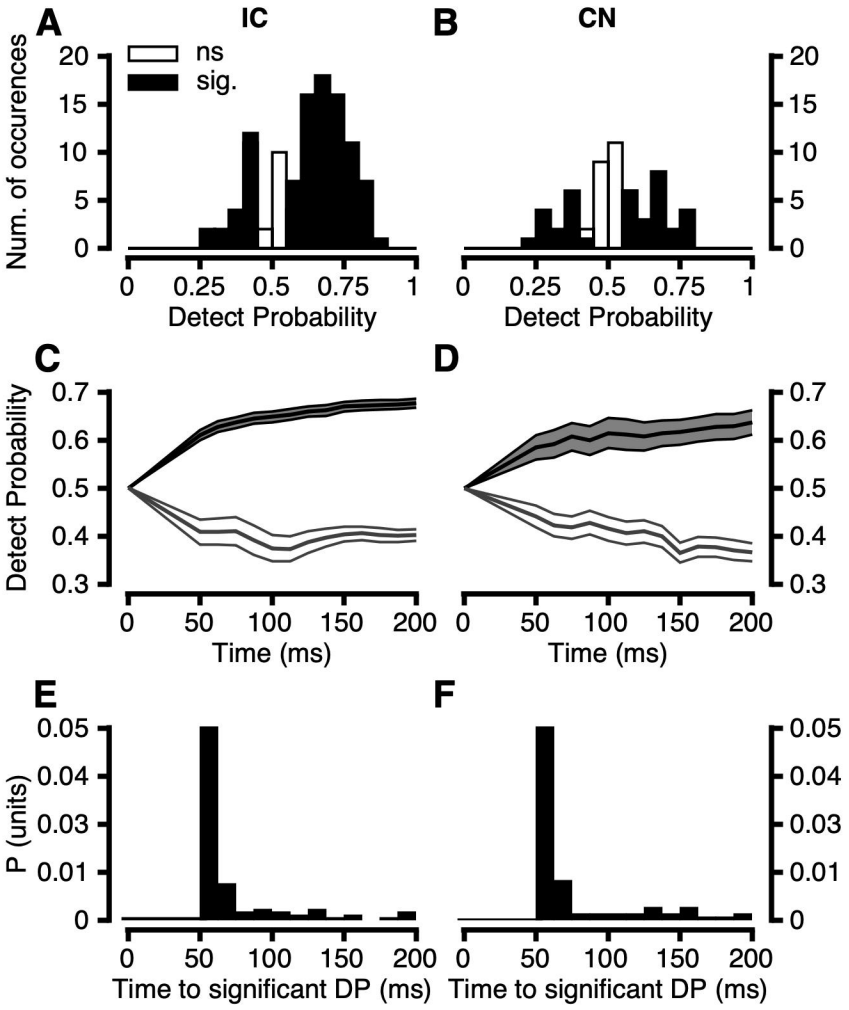
A
IC
ns
sig.
Num. of occurences
20
15
10
5
0
0
0.25
0.5
0.75
1
Detect Probability
B
CN
C
D
Detect Probability
0.7
0.6
0.5
0.4
0.3
0
50
100
150
200
Time (ms)
E
F
P (units)
0.05
0.04
0.03
0.01
Time to significant DP (ms)

1033 **Figure 7**. Relationship between fluctuations in spike count and variations in behavioral response.
1034 A,B. Histogram of detect probability (DP, after Britten et al. 1996; Cook and Maunsell 2002, see
1035 methods for calculation) for all units in the IC (A) and in the CN (B). Black filled bars represent
1036 units that showed a DP significantly different than chance (0.5), as assessed by permutation test
1037 (see Methods). White filled bars represent units with DP values not significantly different from
1038 chance. C,D. Detect Probability (Mean +/- SEM of all units) as a function of time after tone
1039 onset for all units in the IC (C) and the CN (D). Some units' DP increased over time (black error-
1040 bands) while others decreased DP over time (white error-bands). E,F. Proportion histograms of
1041 time elapsing between tone onset and significance of DP in the IC (E) and CN (F).

1042
1043

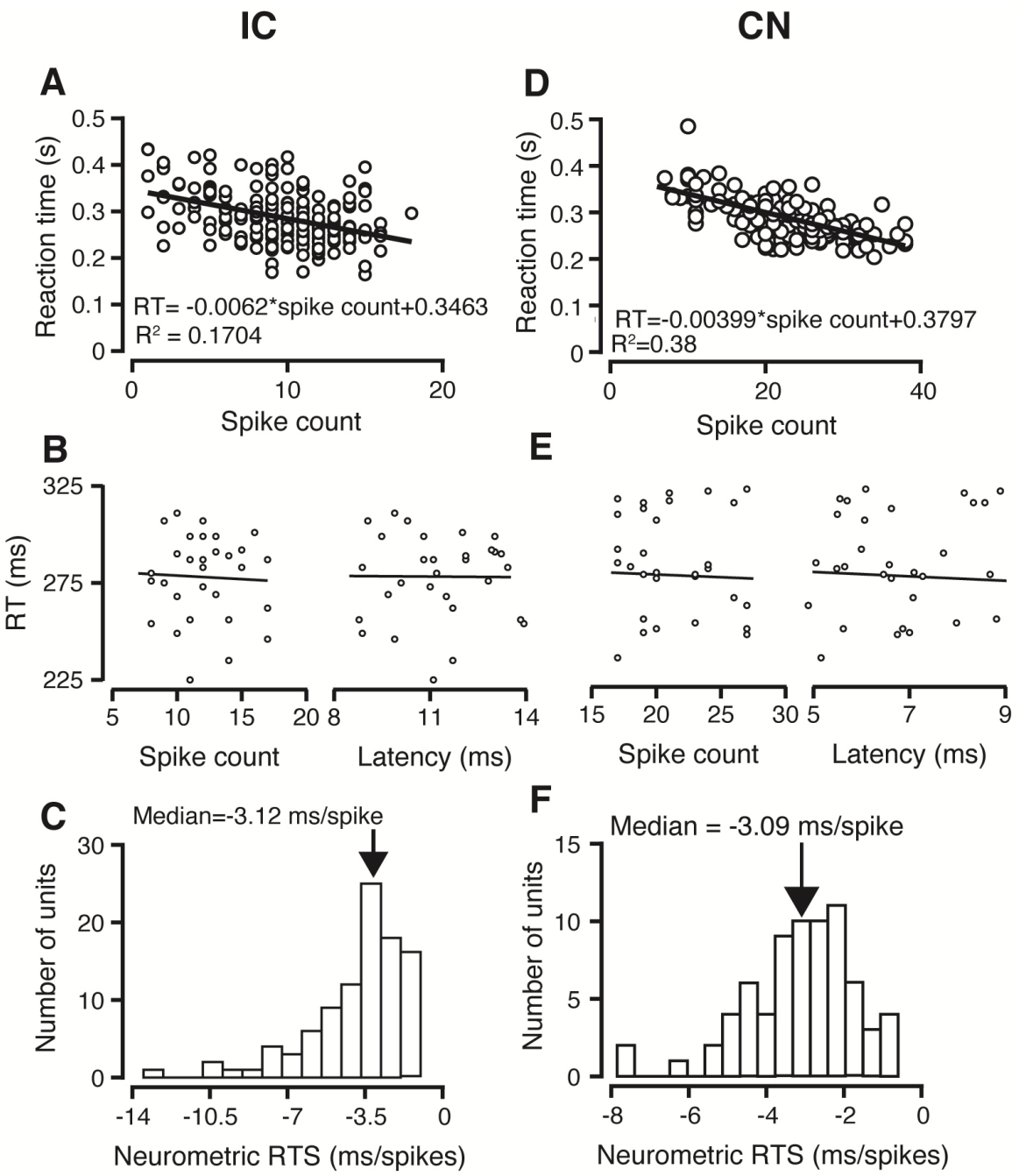

Figure 8. Neuronal correlates of RT in the IC and CN. A, D. Behavioral RT vs. spike count evoked in response to suprathreshold tones for the representative IC type V (A) and CN type I unit (D) whose responses are shown in Figures 2A and 6A. Each symbol represents the RT and the neuronal response on a trial resulting in a lever release. The line represents a linear fit to the data (slope: neurometric RT slope). B, E. Shows RT as a function of spike count (left) and

latency (right) at a fixed sound level in the IC (B) and the CN (E). C, F. Histogram of neurometric RT slope for all IC (C) and CN units (F).

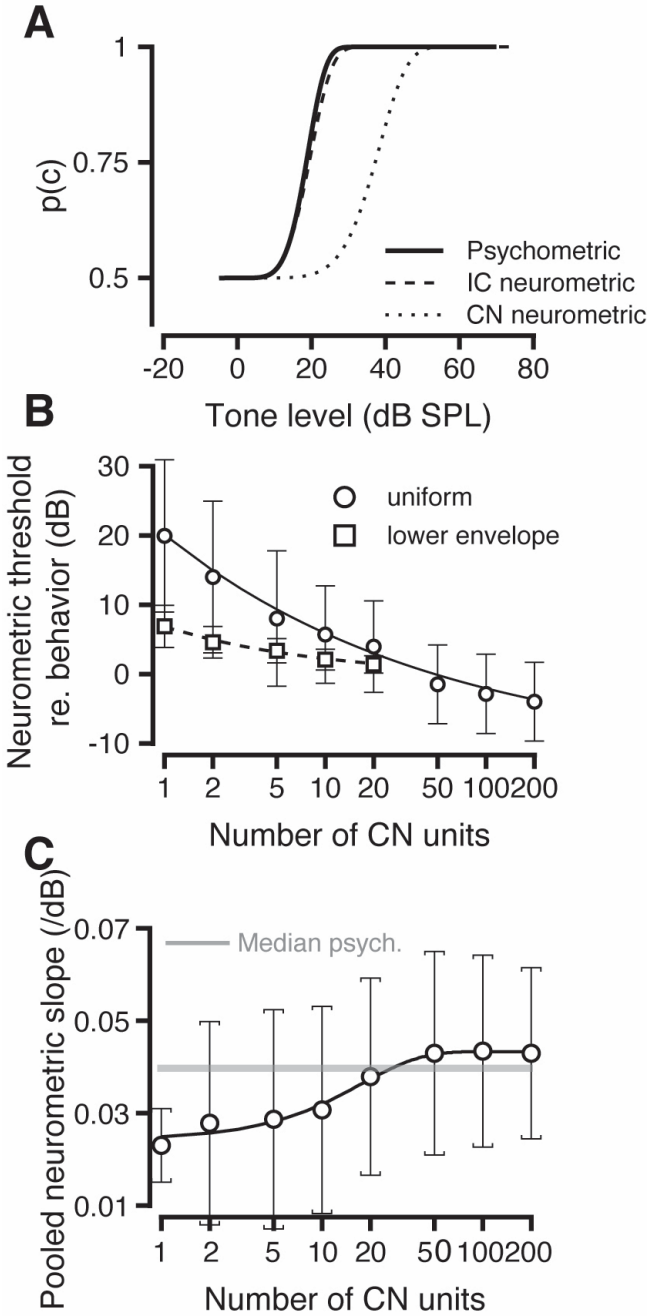

Figure 9. Summary and pooling results. A. Summary of psychometric function (solid lines), IC neurometric functions (dashed), and CN neurometric functions (dotted), illustrating the general finding that IC responses provide better estimates of psychometric

threshold and slope than CN responses. B. Plot of the variation of neurometric thresholds predicted by the combination of different numbers of CN units recorded in this study. Uniform pooling (circles) and lower envelope pooling (squares) strategies are shown. Error bars represent 2 SDs. The solid curve and dashed curve represent power-law fits to the uniform ($\sim N^{-0.22}$) and lower envelope pooling ($\sim N^{-0.41}$). C. Plot of the range of neurometric slopes predicted by the uniform pooling of different numbers of CN units. Error bars represent 2 SDs. Median psychometric slope is shown as a grey line.